QCD EFFECTS IN WEAK RADIATIVE B-MESON DECAYS

Thesis by

Roxanne P. Springer

In Partial Fulfillment of the Requirements
for the Degree of
Doctor of Philosophy

CALIFORNIA INSTITUTE OF TECHNOLOGY
Pasadena, California

1991

(Submitted July 5, 1990)

ACKNOWLEDGMENTS

I thank my advisor Mark Wise for his confidence in me, and for letting me work with him on a very important problem. Ben Grinstein has my thanks for explaining very clearly and patiently what was going on at every stage. I thank D. Politzer for his advice and for explaining to me how physics and physicists fit into the real world. I am grateful to J. Preskill for his beautiful lectures and the time he spent to prepare for us his invaluable lecture notes. I appreciate being treated with much kindness and indulgence by all my friends on the fourth floor, past and present. I thank Martin Savage for discussing with me all his new ideas and dragging me into working on some of them, and for giving me funny looks when I say something stupid.

ABSTRACT

The effective Hamiltonian for $\bar{B}$–meson decays of the form $\bar{B} \to X_s\gamma$, where X_s is a strange hadron, is found in the minimal Standard Model with strong interaction effects included. Renormalization group techniques are used to scale the coefficients of the operators in the effective Hamiltonian to find the inclusive decay rate for hard photon ($E_\gamma \sim 2$ GeV) emission, to leading logarithmic approximation.

TABLE OF CONTENTS

INTRODUCTION

The minimal Standard Model[1.1] has been very successful in predicting and explaining the results seen in high energy particle experiments. The charm and bottom quark have been found, as required by the Standard Model with a minimal Higgs sector for CP violation to exist. The $W^{\pm}$ and Z particles have also been found, as the Standard Model predicted they should be. Yet we know it is not the last word in explaining the events in our universe. There is no motivation for many of its features, nor does it incorporate gravitational interactions. It is certain that the Standard Model, even though quite sufficient to explain physics at the energy scales accessible to us now, will break down at some higher energy scale, where a more complete description of interactions there must be found. In this sense, the Standard Model is an "effective" field theory in its own right. Even astronomical observations that potentially give information on very high energy processes do not yet contradict the Standard Model.

Given that controlled experiments, at energies where we can expect to directly probe the Higgs sector, are far in the future, the best we can do is to look at processes where deviations from the Standard Model will show up most clearly. To this end, the most informative are the decay modes that are predicted to be quite suppressed (relying on heavy virtual particle loops) in the Standard Model, yet have a unique experimental signature.

Among the rare decays of B–mesons are the weak radiative decays, where a B–meson decays to a strange hadronic state X_s and a hard photon γ. Its branching ratio is näively expected at the 10^{-4} level. The decay rate depends on the top quark mass and a measurement of the rate would give a prediction for this mass if the Standard

Model were correct. With the extensive B physics efforts at CESR, and the prospects for future B–meson factories, a measurement of the decay rate could be expected in the next few years. Short distance physics gives rise to an effective magnetic moment type $b \to s\gamma$ interaction. Unlike the analogous process in kaon and hyperon decays (e.g., $K \to \pi\pi\gamma$ and $\Sigma^+ \to p\gamma$) it seems likely that this magnetic moment type interaction dominates the rate for inclusive weak radiative $\bar{B}$–meson decay. If inclusive weak radiative $\bar{B}$ decay is modelled by b–quark decay, then diagrams like Fig. 1 (where a photon is radiated off a quark leg) are, for hard photons, not competitive with the short distance contribution. This is particularly true for very hard photons with $E_\gamma >$ 2 GeV, because then the strange hadronic final state X_s cannot have arisen from the weak decay of a charmed meson. Effects that go beyond the b–quark decay picture are, presumably, suppressed by factors of (Λ/m_b), where Λ is a typical hadronic scale ($\sim$ 300 MeV) and m_b is the b–quark mass.

Since the b–quark is heavy compared with the QCD scale, the short distance contribution to the inclusive $\bar{B} \to X_s\gamma$ decay rate can be approximated by the rate for the free quark decay, $b \to s\gamma$. The narrow width of the $q\bar{q}$ mesons, and the existing data on semileptonic D–decays and semileptonic $\bar{B}$–decays (coming from the $b \to c$ transition) suggest that the final hadronic states X_s are dominated by resonances with $s\bar{q}$ flavor quantum numbers (where q is a u–quark for $\bar{B}^-$ decay and a d–quark for $\bar{B}^0$ decay). The lowest mass $s\bar{q}$ resonance that can contribute is the $K^*(890)$. However, the contribution of this resonance is strongly suppressed by a hadronic form factor, the suppression arising because in the decay $\bar{B} \to K^*\gamma$ a large momentum must be transferred to the "spectator quark" in the recoiling K^* meson (see Fig. 2). In the limit of very large b–quark mass (compared with the typical hadronic scale) the rate is dominated by $s\bar{q}$ resonances with masses of order $m_{X_s} \sim \sqrt{m_b\Lambda}$. For such high mass resonances the typical relative momentum of the quark–antiquark pair is so large that the rate is not suppressed by hadronic form factors. In the large m_b limit, it is these high mass resonances (and not the $K^*(890)$) that dominate the inclusive decay rate given by the free quark decay calculation.

The sensitivity of these radiative decays to new physics makes them an excellent tool for studying extension to the Standard Model. There is no reason for there to exist only one Higgs doublet to give mass to the quarks and leptons. As long as flavor-changing neutral currents remain absent at tree level, the Higgs sector can be made as complicated as desired. In the calculation of the effective $b \to s\gamma$ interaction, loops with virtual top and charm quarks dominate (up quark loops being suppressed by small weak mixing angles); see Fig. 3. In extensions of the standard model with more than one Higgs doublet there are physical charged Higgs bosons that can appear analogous to the charged W–boson in the loop of Fig. 3. The charged Higgs bosons typically couple to quarks proportional to the quark mass. Since the top quark mass is not small (compared with W–boson mass, M_W), processes like $\bar{B} \to X_s\gamma$, where virtual top quarks play an important role, are particularly sensitive to the structure of the Higgs sector [1.2].

In this thesis, a detailed discussion of the leading logarithmic strong interaction corrections to the effective Hamiltonian for weak radiative $\bar{B}$–meson decay in the Standard Model will be given. With this result, it is clear how effects of extensions to the Standard Model can be incorporated, though this is not done here. In fact, it is somewhat inappropriate to call these leading logarithmic strong interaction effects "corrections." Although $[\alpha_s(m_b)/\pi]$ is small, $[\alpha_s(m_b)/\pi]\ell n(m_t^2/m_b^2)$ is not small and so all the leading logarithmic terms of the form$\{[\alpha_s(m_b)/\pi]\ell n(m_t^2/m_b^2)\}^p$ should be summed (using the renormalization group) in order to get the correct effective

Hamiltonian. Even if these alter the free quark result (that follows from Fig. 3) significantly, we expect the next–to–leading logarithmic effects to be only a small correction.

Chapter 1 reviews the Standard Model and comments on the techniques of effective field theories and the renormalization group. Chapter 2 contains a discussion of the operator basis appropriate for the effective Hamiltonian for weak radiative $\bar{B}$–meson decay. The coefficients of the operators in this effective Hamiltonian are evaluated in the minimal Standard Model, with a subtraction point approximately equal to the W–boson mass. Chapter 3 contains the derivation of the anomalous dimension matrix, which is used to scale the coefficients of the operators down to a subtraction point about equal to the b–quark mass. This procedure transfers the large logarithms from the matrix elements of the operators to their coefficients. For the anomalous dimension matrix, two-loop graphs are important. Because of this it is necessary to treat the matrix γ_5 correctly. The appendix of ref.[1.3] contains a justification of the treatment of γ_5 used here. In solving the renormalization group equations, a truncated form of the anomalous dimension matrix is used. Chapter 4 contains a detailed discussion of the accuracy of this truncation. Finally, in Chapter 5, we present results for the inclusive $\bar{B} \to X_s\gamma$ rate.

The early results given here were published (with Mark B. Wise and Benjamin Grinstein) in *Physics Letters* **B202**, 138 (1988), and presented at the Twenty-Fourth International Conference on High Energy Physics in Munich, 1988. Included in *Proceedings of the XXIV International Conference on High Energy Physics*, ed. R. Kotthaus and J.H. Köhn, (Springer Verlag, 1988), p. 573, is a brief discussion on the validity of using the truncated form of the anomalous dimension matrix. The final paper is to be published in *Nuclear Physics* **B**.

Chapter 1. Some Tools

In order to calculate the strong interaction corrections to weak radiative B meson decay, it is necessary to know the Feynman rules with which to calculate the appropriate Feynman graphs. The starting point for this is the Standard Model, and so it is reviewed here. To obtain and use a set of nonrenormalizable operators to calculate the rate in an effective theory, something about the technique of effective field theories is needed. The renormalization group is used to take into account how the operators in the effective theory change as the energy scale changes.

1.1 The Standard Model

The minimal Standard Model[1.1,1.4] provides a scheme for understanding the strong, weak, and electromagnetic forces between particles. Particle content consists of three generations of quarks and leptons arranged in left-handed doublets and right-handed singlets. Each quark is a color triplet, occurring, for example, in red, blue, and green. The fermions in the theory are the leptons

$$L_L^i = \begin{pmatrix} \nu^i \\ l^i \end{pmatrix}_L \qquad l_R^i, \tag{1.1.1}$$

and the quarks

$$Q_L^i = \begin{pmatrix} u^i_{Red} \\ d^i_{Red} \end{pmatrix}_L, \begin{pmatrix} u^i_{Blue} \\ d^i_{Blue} \end{pmatrix}_L, \begin{pmatrix} u^i_{Green} \\ d^i_{Green} \end{pmatrix}_L. \tag{1.1.2}$$

$$(u^i_{Red})_R, \quad (u^i_{Blue})_R, \quad (u^i_{Green})_R, \quad (d^i_{Red})_R, \quad (d^i_{Blue})_R, \quad (d^i_{Green})_R. \tag{1.1.3}$$

The index i runs over the three generations so that, for example, $l_R^1 = e_R$ and $d_L^3 = b_L$. The up quarks are the u^i and the down quarks are the d^i. The subscript L denotes the left-handed component of the fermion so that, for example, $u_L = \frac{1}{2}(1 - \gamma^5)u$, and R labels the right-handed fermions. With the neutrino taken as massless, it has no right-handed part; $\nu_R = \frac{1}{2}(1 + \gamma_5)\nu = 0$. To include electromagnetism, the weak hypercharge Y is defined such that $Q = I_3 + \frac{1}{2}Y$, where I_3 is the third component of the weak isospin under which the left handed fermions transform as doublets, and Q is the conserved charge of the fermion.

Mass is given to the gauge bosons W^+, W^-, and Z^0, the mediators of the weak force, by the presence of the scalar Higgs[1.5] doublet $\phi = \binom{\phi^+}{\phi^0}$. This doublet spontaneously breaks the full gauge symmetry $SU(3)_c \times SU(2)_L \times U(1)_Y$ of the model to the $SU(3)_c \times U(1)_Y$ seen at energies below 100 GeV. $SU(3)_c$ is the color group, $SU(2)_L$ is the weak isospin group, and $U(1)_Y$ is the weak hypercharge group. Table 1.1 summarizes the transformation properties of the matter fields in the minimal Standard Model.

Table 1.1: Matter fields in the Standard Model

Field	$SU(3)_c$	$SU(2)_L$	$U(1)_Y$	Spin
$Q^i_L = \binom{u^i_L}{d^i_L}$	3	2	1/3	1/2
u^i_R	3	1	4/3	1/2
d^i_R	3	1	-2/3	1/2
$L^i_L = \binom{\nu^i_L}{l^i_L}$	1	2	-1	1/2
l^i_R	1	1	-2	1/2
$\phi = \binom{\phi^+}{\phi^0}$	1	2	1	0

The gauge bosons associated with $SU(2)_L$ are W^1_μ, W^2_μ, and W^3_μ, where $\mu = 1, 2, 3, 4$ is the Dirac index. The gauge boson for the $U(1)_Y$ group is B_μ. Then the kinetic energy term in the Lagrangian for the electroweak sector is

$$\mathcal{L} = -\frac{1}{4}F^a_{\mu\nu}F^{a\mu\nu} - \frac{1}{4}f_{\mu\nu}f^{\mu\nu}, \tag{1.1.4}$$

where $F^a_{\mu\nu}$ and $f_{\mu\nu}$ are the field strength tensors for $SU(2)_L$ and $U(1)_Y$, respectively. At this point, there are four massless gauge bosons in W^a_μ and B_μ. However, it is known that only the photon field is massless in reality. Also, the global $SU(2)$ invariance prohibits mass terms for the quarks and leptons. To obtain a theory with massive fermions and a single conserved quantity Q associated with one massless gauge boson, the complex scalar ϕ is used. Then a term in the Lagrangian for the Higgs sector must be included:

$$\mathcal{L}_H = (D^\mu\phi)^\dagger(D_\mu\phi) - V(\phi^\dagger\phi), \tag{1.1.5}$$

where the covariant derivative in the electroweak sector is

$$D_\mu = \partial_\mu + i\frac{g_1}{2}B_\mu Y + i\frac{g_2}{2}\sigma^a W^a_\mu. \tag{1.1.6}$$

The generator of the weak hypercharge is Y and the generators of $SU(2)_L$ are the $T^a = \frac{1}{2}\sigma^a$, a=1,2,3, with the Pauli matrices

$$\sigma^1 = \begin{pmatrix} 0 & 1 \\ 1 & 0 \end{pmatrix}, \quad \sigma^2 = \begin{pmatrix} 0 & -i \\ i & 0 \end{pmatrix}, \quad \sigma^3 = \begin{pmatrix} 1 & 0 \\ 0 & -1 \end{pmatrix}. \tag{1.1.7}$$

To allow spontaneous symmetry breaking of the $SU(2)_L$ group, the potential used is:

$$V(\phi^\dagger\phi) = \frac{\lambda}{4}(\phi^\dagger\phi - v^2)^2. \tag{1.1.8}$$

This gives the "Mexican hat" potential form with a well of potential minima in a circle of radius v about the origin in the complex ϕ plane. It is also possible to include an interaction term for the Higgs scalars and fermions using the Yukawa coupling. This gives a term in the Lagrangian that generates a mass for the quarks and leptons:

$$\mathcal{L}_Y = g_u^{ij}\overline{u}_R^i\phi^T\epsilon Q_L^j + g_d^{ij}\overline{d}_R^i\phi^\dagger Q_L^j + g_l^{ij}\overline{l}_R^i\phi^\dagger L_L^j + h.c. \tag{1.1.9}$$

The indices i and j are summed over the three generations, and the color indices are understood. g_u, g_d, and g_l are the coupling matrices for the up-type quarks, the down-type quarks, and the leptons, respectively.

$$\epsilon = \begin{pmatrix} 0 & 1 \\ -1 & 0 \end{pmatrix} \tag{1.1.10}$$

is the totally antisymmetric ϵ matrix.

Choosing a vacuum expectation value for the Higgs doublet breaks the $SU(2)_L$ symmetry. Let $\langle\phi\rangle_0 = \binom{0}{v}$ and then expand about this value to see how $\mathcal{L}_H$ and $\mathcal{L}_Y$ behave. First notice that the vacuum is invariant under a generator G if

$$e^{i\alpha G}\langle\phi\rangle_0 = \langle\phi\rangle_0. \tag{1.1.11}$$

To first order in α this becomes

$$(1 + i\alpha G)\langle\phi\rangle_0 = \langle\phi\rangle_0. \tag{1.1.12}$$

or

$$G\langle\phi\rangle_0 = 0. \tag{1.1.13}$$

For the generators in the electroweak sector:

$$\sigma^1\langle\phi\rangle_0 = \begin{pmatrix} 0 & 1 \\ 1 & 0 \end{pmatrix}\binom{0}{v} = \binom{v}{0} \neq 0, \tag{1.1.14a}$$

$$\sigma^2\langle\phi\rangle_0 = \begin{pmatrix} 0 & -i \\ i & 0 \end{pmatrix}\begin{pmatrix} 0 \\ v \end{pmatrix} = \begin{pmatrix} -iv \\ 0 \end{pmatrix} \neq 0, \tag{1.1.14b}$$

$$\sigma^3\langle\phi\rangle_0 = \begin{pmatrix} 1 & 0 \\ 0 & -1 \end{pmatrix}\begin{pmatrix} 0 \\ v \end{pmatrix} = \begin{pmatrix} 0 \\ -v \end{pmatrix} \neq 0, \tag{1.1.14c}$$

$$Y\langle\phi\rangle_0 = \begin{pmatrix} 1 & 0 \\ 0 & 1 \end{pmatrix}\begin{pmatrix} 0 \\ v \end{pmatrix} = \begin{pmatrix} 0 \\ v \end{pmatrix} \neq 0. \tag{1.1.14d}$$

But it is apparent that the combination can be chosen so that

$$Q\langle\phi\rangle_0 = \frac{1}{2}\left(\sigma^3 + Y\right)\langle\phi\rangle_0 = 0, \tag{1.1.15}$$

so that Q is the generator of the unbroken symmetry, and we get the conserved quantity Q and the massless photon field associated with it.

Because of the vacuum expectation value given to the Higgs doublet, there are now mass terms in L_Y such that:

$$m_u = vg_u, \quad m_d = -vg_d, \quad \text{and} \quad m_l = -vg_l, \tag{1.1.16}$$

where m_u, m_d, and m_l are the up-type quark, the down–type quark, and the lepton 3×3 mass matrices, respectively. Unitary transformations on the left– and right–handed fermion fields give the familiar diagonal mass matrices. With unitary matrices $T_L, T_R, V_L, V_R, W_L, \text{and} W_R$, then

$$u^i_{L,R} = T^{ij}_{L,R}(u')^j_{L,R} \tag{1.1.17a}$$

$$d^i_{L,R} = V^{ij}_{L,R}(d')^j_{L,R} \tag{1.1.17b}$$

$$l^i_{L,R} = W^{ij}_{L,R}(l')^j_{L,R}, \tag{1.1.17c}$$

with i,j=1,2,3 and the primed fields are the mass eigenstates. The diagonalized matrices can then be written as

$$T_R^\dagger m_u T_L = \begin{pmatrix} m_u & 0 & 0 \\ 0 & m_c & 0 \\ 0 & 0 & m_t \end{pmatrix} \tag{1.1.18a}$$

$$V_R^\dagger m_d V_L = \begin{pmatrix} m_d & 0 & 0 \\ 0 & m_s & 0 \\ 0 & 0 & m_b \end{pmatrix} \tag{1.1.18b}$$

$$W_R^\dagger m_l W_L = \begin{pmatrix} m_e & 0 & 0 \\ 0 & m_\mu & 0 \\ 0 & 0 & m_\tau \end{pmatrix}. \tag{1.1.18c}$$

The gauge bosons acquire mass through the kinetic energy terms in $\mathcal{L}$. At the vacuum expectation value:

$$\mathcal{L}_{gauge\ mass} = \frac{v^2}{4}\Big((g_1 B_\mu - g_2 W_\mu^3)^2 + g_2^2 |W_\mu^1 + iW_\mu^2|^2\Big). \tag{1.1.19}$$

To find the charged mass terms we can define:

$$W_\mu^\pm \equiv \frac{1}{\sqrt{2}}(B_\mu^1 \mp iB_\mu^2), \tag{1.1.20}$$

so that the charged vector boson piece becomes

$$\frac{g_2^2 v^2}{4}(|W_\mu^+|^2 + |W_\mu^-|^2), \tag{1.1.21}$$

and the mass is:

$$M_W^\pm = g_2 v. \tag{1.1.22}$$

To find the neutral boson masses we define the orthogonal combinations:

$$Z_\mu = \cos\theta_W W_\mu^3 - \sin\theta_W B_\mu \tag{1.1.23}$$

and

$$A_\mu = \cos\theta_W B_\mu + \sin\theta_W W_\mu^3, \tag{1.1.24}$$

where

$$\sin\theta_W = \frac{g_1}{\sqrt{g_1^2 + g_2^2}}, \quad \cos\theta_W = \frac{g_2}{\sqrt{g_1^2 + g_2^2}}, \tag{1.1.25}$$

so that we can isolate the neutral Z boson that acquires a mass $M_Z = \frac{M_W}{cos\theta_W}$, and see that the photon field A_μ remains massless. Now, with the generators $T_\pm = \frac{\sigma_\pm}{2}$, and $\sigma_\pm = (\sigma_1 \pm i\sigma_2)/\sqrt{2}$, the covariant derivative in terms of the mass eigenstate gauge fields becomes

$$D^\mu = \partial^\mu + \frac{ig_2}{2}\sigma_+ W_+^\mu + \frac{ig_2}{2}\sigma_- W_-^\mu \ + \ iQg_2\sin\theta_W A^\mu$$

$$+ \frac{i}{2}\sqrt{g_1^2 + g_2^2}(\sigma_3 - 2Q\sin^2\theta_W)Z^\mu, \tag{1.1.26}$$

and then the electromagnetic coupling constant is identified as

$$e = g_2 \sin\theta_W. \tag{1.1.27}$$

To get the couplings (and thereby the Feynman rules with which to evaluate Feynman diagrams) of the boson fields to the quarks, we look at the kinetic energy term for the left-handed quarks, written in terms of the mass eigenstate quark fields:

$$i(\overline{u}')^j_L\gamma_\mu\Big(\partial^\mu + i\sqrt{g_1^2+g_2^2}\Big(\frac{1}{2}-\frac{2}{3}\sin^2\theta_W\Big)Z^\mu + ie\Big(\frac{2}{3}\Big)A^\mu\Big)(u')^j_L$$

$$+i(\overline{d}')^j_L\gamma_\mu\Big(\partial^\mu + i\sqrt{g_1^2+g_2^2}\Big(-\frac{1}{2}+\frac{1}{3}\sin^2\theta_W\Big)Z^\mu + ie\Big(-\frac{1}{3}\Big)A^\mu\Big)(d')^j_L$$

$$-\frac{g_2}{\sqrt{2}}\Big((\overline{u}')^j_L\gamma_\mu K^{jm}(d')^m_L W^\mu_+ + h.c.\Big). \tag{1.1.28}$$

The color indices are suppressed and repeated indices are summed over the three generations of quarks. Note that there are no tree level flavor-changing neutral currents. The Kobayashi-Maskawa[1.6] matrix in terms of the unitary matrices that diagonalized the quark mass matrices is $K = T_L^\dagger V_L$. For three generations in the Standard Model, K is often parameterized by four angles θ_1, θ_2, θ_3, and δ so that

$$K = \begin{pmatrix} c_1 & -s_1c_3 & -s_1s_3 \\ s_1c_2 & c_1c_2c_3 - s_2s_3e^{i\delta} & c_1c_2s_3 + s_2c_3e^{i\delta} \\ s_1s_2 & c_1s_2c_3 + c_2s_3e^{i\delta} & c_1s_2s_3 - c_2c_3e^{i\delta} \end{pmatrix}. \tag{1.1.29}$$

The abbreviated $c_i \equiv \cos\theta_i$ and $s_i \equiv \sin\theta_i$, with i=1,2,3. If the quark masses remain nondegenerate and none of the angles θ_i vanish, it is not possible to make K real.

So by allowing the Higgs doublet to obtain a vacuum expectation value, the $SU(3)_c \times SU(2)_L \times U(1)_Y$ theory for quarks and leptons has been spontaneously broken to yield mass terms for these fermions and the intermediate vector bosons $W^\pm_\mu$ and Z_μ. However, there is another result that comes out of this procedure. With the field redefinitions $\phi^+ \to h^+$ and $\phi^0 \to v + h^0$, the potential in the Higgs portion of the Lagrangian becomes

$$V_H = \frac{\lambda}{4}(h^{+*}h^+ + h^{0*}h^0 + 2vReh^0)^2. \tag{1.1.30}$$

This means that there is a real massive scalar Reh^0 with a mass

$$m_{Reh^0} = \sqrt{\lambda}v. \tag{1.1.31}$$

This has yet to be confirmed by experiment.

1.2 Effective Field Theories

In some ways, the idea behind effective field theories is one that is quite fundamental to our belief that physics can be studied at all[1.7]. We have to assume, at each level of knowledge, that it is possible to find out something about the laws that govern our world without knowledge of how *everything* works at all levels. We have to assume that we can study e^+e^- collisions and learn what we can expect to see happen at those energy scales and have a theory that is predictive there, without knowing how the interactions behave at energies at the Planck mass scale. This means that if we are interested in what happens at some scale μ, we *don't* need to have full information about what happens at some scale $\Lambda >> \mu$. The information needed about those high energy scales will be incorporated into coupling constants and particle masses that are seen at scale μ.

Probably, all the theories that we now accept as the current best are effective theories in the above sense (except, perhaps, superstring theory). But it often happens that to make a problem more tractable, it is judicious to "throw away" some information we have about our theory and obtain an effective field theory as the framework in which to do the calculation. This is loosely analogous to statistical mechanics where, to find the volume or pressure of a box full of atoms, it is better *not* to know all the microscopic information on individual particle locations and momenta, but work only with "averages" of such quantities. In the words of Howard Georgi, the use of effective field theories "will make hard calculations easy and impossible calculations doable."

To incorporate all of the information about a full theory into an effective theory would require an infinite number of nonrenormalizable operators involving an infinite number of parameters. This would seem to be a step backwards. However, if we know the full underlying theory, it is possible to calculate all of these parameters. Further, the dimensionful parameters that appear in this infinite list will all involve powers of the masses of the heavy particles of the full theory. When these masses are very large compared to the energy scale we are calculating in, the effect of many of the nonrenormalizable operators will be highly suppressed. This process can give much qualitative insight into the problem we are calculating. An effective field theory will contain operators and a coefficient for each of them. The matrix element of these operators will typically contain large logarithms, which would make them difficult to calculate. However, by renormalizing the theory, as discussed in the next section, we can move the large logarithms from the matrix elements into the coefficients of the operators. These coefficients we can then calculate, and the matrix elements will have no large logarithms and will therefore be amenable to lattice theory calculations.

As we look at increasingly higher energies, each new particle that appears can be interpreted as introducing a new effective field theory. They are the "new physics" that must now be incorporated into the theory. To match the new effective theory onto the old one it is sufficient to require that, just below the threshold for making the new particle, the two theories give identical results. This essentially requires that the coupling constants for the particles existing in both theories will be continuous across the boundary into the theory containing new particles. The conditions that satisfy the above are called the "matching conditions" of the theory. For them to be calculated using perturbation theory, they are evaluated at the scale μ near the boundary mass between the two.

In this way, we do not need to know what the full renormalizable theory is or whether it in fact exists. The more stringent requirement of renormalizability is then replaced, at this level, with conditions on the effective theories. If nonrenormalizable operators are present that have couplings of $1/M$ to a power, where $M > \mu$, then we know that there exist particles in the theory with mass m on the order of M in order to account for these operators. When the effective theory is found that is valid at energies $\mu > m$, it must include these particles. As we go up in energy towards higher mass particles, the nonrenormalizable operators in the effective theory valid below these energies become more important until they must be replaced by operators that respect the finite nature of the new particle masses.

Moving in the opposite direction, if we have a theory valid at higher energies, a calculation at lower energies is often easier if we remove from the theory the information that does not affect our calculation. A nice example of this is given in ref.[1.8], where an effective field theory useful for calculations in kaon decays was found by stepwise removing first the W boson and then the heavy quarks, one by one.

1.3 The Renormalization Group[1.9]

In order to calculate the $b \to s\gamma$ decay rate, we need to be able to find the value of the coefficients of the operators in our effective theory at about the bottom mass scale,

$C_j(m_b)$, from knowledge of their value at the W mass scale, $C_j(M_W)$. The coefficients at the W mass scale are found using matching conditions. The renormalization group equations tell us how to find the $C_j(m_b)$ from the $C_j(M_W)$.

To illustrate how this may occur, we can look at QCD interactions without quarks; in particular the interaction between two static color sources. The energy involved is proportional to g^2, where g is the QCD coupling constant. At the classical level, there is no mass scale set by QCD, yet this does not survive to the quantum theory. The reason is that the medium can polarize in the same way that it polarizes in the presence of electric charge. In QED, vacuum polarization has the effect of "screening" an electron so that its "bare" coupling constant is not the same as its "renormalized" (screening taken into account) value. The same process can occur in QCD, only now the vacuum fluctuations are virtual gluon pairs, and the coupling constant changes value or "runs," as it does in QED. Since this screening occurs, the coupling constant g should be a function of separation of the color sources, r. However, the coupling is also dimensionless (when $\hbar = \mathrm{c} = 1$) and so the energy $\mathrm{E} \sim g^2(\mathrm{r}) = g^2(\mu\, \mathrm{r})$, and now a mass scale has appeared. This means that when calculating an interaction process in QCD, the loop corrections give logarithmic ultraviolet divergences that must be subtracted away. This subtraction is done at a mass scale μ. Under the renormalization group, such a scale is needed to define the renormalized Green's functions (the result of Feynman diagram evaluation), but all physical results must be *independent* of this mass scale. This is what is meant by saying it may be chosen arbitrarily. The movement of this scale μ in the theory is accomplished using renormalization group equations.

Consider a scalar field theory, where field renormalization is given by $Z_i(\mu)$ and the renormalized coupling is g_μ. These quantities are dependent on the subtraction point μ so that physics can be made independent of μ. An n-point Green's function (renormalized) in this theory is

$$G_R^{(n)} = < 0|T[\phi_R ... \phi_R]|0 >, \tag{1.3.1}$$

where T is the time-ordering operator. This Green's function is a function of a g_μ, and μ, among other things:

$$G_R^{(n)} = G_R^{(n)}(g_\mu, \mu). \tag{1.3.2}$$

The bare, unrenormalized Green's functions are independent of μ, and are functions of the bare coupling constant, g_o, and a cutoff Λ. The cutoff, Λ, is needed so that the calculations done with unrenormalized Green's functions are finite.

$$G_U^{(n)} = G_U^{(n)}(g_o, \Lambda). \tag{1.3.3}$$

We can use the μ independence of these functions to obtain the scaling law. The relation between the two forms is:

$$g_\mu = g_\mu(g_o, \Lambda), \tag{1.3.4}$$

$$G_R^{(n)}(g_\mu, \mu) = [Z(\frac{\Lambda}{\mu})]^{-n/2} G_U^{(n)}(g_o, \Lambda). \tag{1.3.5}$$

This means that the quantity

$$[Z(\frac{\Lambda}{\mu})]^{n/2} G_R^{(n)}(g_\mu, \mu) \tag{1.3.6}$$

is independent of μ. So, picking $\mu = E$, we have

$$[Z(\mu)]^{n/2} G_R^{(n)}(g_\mu, \mu) = [Z(E)]^{n/2} G_R^{(n)}(g_E, E), \tag{1.3.7}$$

or,

$$G_R^{(n)}(g_\mu, \mu) = \left[\frac{Z(E)}{Z(\mu)}\right] G_R^{(n)}(g_E, E). \tag{1.3.8}$$

This is the integrated form of the renormalization group equation, and shows that by finding $Z(\mu)$ and g_μ, we can determine the scaling law for the Green's function. The Green's functions will have contributions from logarithms whose arguments are the typical mass scale, E, divided by the subtraction point, μ. Choosing $\mu = E$ removes the large logarithms from the matrix elements. This is why we use the renormalization equations.

Alternatively, consider a field theory with field renormalization $Z(\mu)$ and renormalized coupling constant g_μ. The theory does have a mass scale, as before, but it is arbitrary. So

$$g_{\mu'} = g_{\mu'}(\frac{\mu'}{\mu}, g_\mu). \tag{1.3.9}$$

Differentiating with respect to μ' and then setting $\mu' = \mu$ gives

$$\mu \frac{d}{d\mu} g_\mu = \beta_\mu, \tag{1.3.10}$$

where β is a function of g_μ alone. Also,

$$Z(\mu')^{1/2} = Z(\mu)^{1/2} F(\frac{\mu'}{\mu}, g_\mu). \tag{1.3.11}$$

Again, differentiating with respect to μ' and setting $\mu' = \mu$, yields:

$$\mu \frac{d}{d\mu} ln Z(\mu)^{1/2} = \gamma(g_\mu), \tag{1.3.12}$$

were γ is another function of g_μ only. Then the μ independence of the unrenormalized

Green's function:

$$\mu\frac{d}{d\mu}[Z(\mu)]^{n/2}G_R^{(n)}(g_\mu,\mu) = 0. \tag{1.3.13}$$

can be expressed as:

$$[\mu\frac{\partial}{\partial\mu} + \beta(g_\mu)\frac{\partial}{\partial g_\mu} + n\gamma(g_\mu)]G_R^{(n)} = 0. \tag{1.3.14}$$

Determining the functions β and γ will determine how the Green's functions scale with energy. To find β and γ, one must find g_μ and $Z(\mu)$, usually perturbatively, which is what will be done here.

The scaling of mass terms is done in the same way. If it is treated as a coupling constant dependent on the subtraction point, μ, the Green's function is now a function of the quantity $\frac{m(\mu)}{\mu}$ and

$$\gamma_m = \frac{1}{2}\mu\frac{d}{d\mu}ln(m^2) \tag{1.3.15}$$

gives the scaling behavior.

References for the Introduction and Chapter 1

1.1. S.L. Glashow, Nucl. Phys. **22** (1961) 579; S. Weinberg, Phys. Rev. Lett. **19** (1967) 1264; A. Salam, in *Elementary Particle Physics: Relativistic Groups and Analyticity*, Nobel Symp. No. 8, ed. N. Svartholm (Almqvist and Wiksell, Stockholm, 1968), p. 367.

1.2. B. Grinstein and M.B. Wise, Phys. Lett. **B201** (1988) 274; W.-S. Hou and R. Willey, Phys. Lett. **B202** (1988) 591.

1.3. B. Grinstein, M. Savage and M.B. Wise, Nucl. Phys. **B319** (1989) 271.

1.4. A nice review is given in M.B. Wise, *CP Violation*, given at the Banff Summer Institute, Aug. 14-27 (1988).

1.5. P. W. Higgs, Phys. Lett. **12** (1964) 132; Phys. Lett. **13** (1964) 508.

1.6. M. Kobayashi and T. Maskawa, Prog. Theor. Phys. **49** (1973) 652.

1.7. From discussions in J. Preskill's lectures in field theory, Caltech, 1987-90; and H. Georgi *Weak Interactions and Modern Particle Theory* (Benjamin/Cummins, 1984).

1.8 F. Gilman and M. Wise, Phys. Rev. **D20** (1979) 2392.

1.9. From discussions in J. Preskill's lectures in field theory, Caltech, 1987-90; H.D Politzer, Physics Reports **14C** (1974) 129; D. Gross and F. Wilczek, Phys. Rev. **D8** (1973) 3633; **D9** (1974) 980; D. Gross, *Les Houches Lectures, 1975, Methods in Field Theory*, ed. R. Balian and J. Zinn-Justin (North-Holland, 1976), and references therein.

Chapter 2. Matching Conditions

We want to find an effective Hamiltonian for the $b \to s\gamma$ decay. This is done by "integrating out" the heavy degrees of freedom in the full theory to obtain the (non-renormalizable) operators that will mimic the effect of the full theory at the energy scales we are interested in. This is analogous to approximating the intermediate W boson exchange in β decay by the four fermi point interaction found by taking the W mass to infinity and noting that at low enough energy scales the finiteness of the W mass is irrelevant. This standard procedure[2.1] will incorporate into appropriate coefficients the information removed. For our case the heavy particles in question are the top quark and W boson in the Standard Model. For a theory with a more complicated Higgs structure, the charged scalars will also be removed. In supersymmetric theories there will be heavy partners to the standard particles that can contribute to the $b \to s\gamma$ decay rate, which should be removed to form an effective Hamiltonian valid under supersymmetry. The phrase "integrating out" arises from the path integral formalism where one is formally integrating over the degrees of freedom associated with the heavy particles and is therefore left with a nonrenormalizable (unsymmetrically weighted) function of the remaining degrees of freedom. In practice, the procedure amounts to evaluating the relevant Feynman diagrams and extracting the piece of the diagram that contributes to an operator in the effective Hamiltonian. This piece determines the coefficient of the operator at the energy scale of the particles removed and is called the matching condition.

We want to integrate out the heavy particles (i.e., the top quark and the W–boson in the Standard Model with minimal Higgs sector) in order to derive an effective Hamiltonian for weak radiative $\bar{B}$–meson decay. This effective Hamiltonian is expressible in terms of the "light" u, d, s, c and b–quark fields and the photon and gluon fields. The effective Hamiltonian can contain local operators, O_j, of arbitrarily high dimension, d_j, which are invariant under the unbroken color and electromagnetic gauge interactions. The resulting Hamiltonian must be of dimension four, however (to leave the corresponding action dimensionless; $\hbar$=c=1), so higher dimension operators are suppressed by powers of the masses of the heavy particles that were integrated out. Also, renormalizable operators with dimension $d_j \leq 4$ are not relevant because they are flavor off–diagonal mass or kinetic terms that are removable by field redefinitions (i.e., they renormalize the values of the quark masses and the weak mixing angles). Therefore it is nonrenormalizable operators of the lowest possible dimension that dominate the effective Hamiltonian.

To derive the effective Hamiltonian in the Standard Model with minimal particle content [2.2], one integrates out the heavy W–boson and top quark. The couplings of the heavy fields to the light fields are given by the interaction Lagrangian density

$$\mathcal{L} \;=\; -\frac{g_2}{\sqrt{2}}\,(\bar{u},\bar{c},\bar{t})_L\,\gamma^\mu\,V\begin{pmatrix} d \\ s \\ b \end{pmatrix}_L W_\mu^+ \;+\; \text{h.c.} \tag{2.1}$$

Here the Kobayashi–Maskawa matrix, V, is a 3×3 unitary matrix that arises from diagonalization of the quark mass matrices. It is possible to express V in terms of four angles θ_1, θ_2, θ_3, and δ, in the following way [2.3]

$$V \;=\; \begin{pmatrix} c_1 & -s_1c_3 & -s_1s_3 \\ s_1c_2 & c_1c_2c_3 - s_2s_3e^{i\delta} & c_1c_2s_3 + s_2c_3e^{i\delta} \\ s_1s_2 & c_1s_2c_3 + c_2s_3e^{i\delta} & c_1s_2s_3 - c_2c_3e^{i\delta} \end{pmatrix}, \tag{2.2}$$

where $c_i \equiv \cos\,\theta_i$ and $s_i \equiv \sin\,\theta_i$ for $i = 1,2,3$. Without loss of generality the angles θ_1, θ_2, and θ_3 are chosen to lie in the first quadrant, where their sines and cosines are positive. Then the quadrant of the angle δ has physical significance and cannot be chosen by convention. Experimental information on kaon decays, nuclear β–decay, hyperon decays and $\bar{B}$–meson decays implies that the angles θ_1, θ_2, and θ_3 are small [2.4].

It is the interaction (2.1) that determines, in the minimal Standard Model, the flavor quantum numbers of the effective Hamiltonian for weak radiative $\bar{B}$–meson decay. To form an effective theory for the $b \to s$ decay we want to find all possible dimension five and dimension six operators that could contribute to this process. Operators of higher dimension will be suppressed by more orders of the heavy mass. The dimension six operators are competitive with those of dimension five since the dimension five operators all appear with a factor of m_b in them, which makes them effectively of dimension six for counting the powers of heavy masses that appear in the denominator of the operator. The matching conditions will be found at a subtraction point μ that is much greater than m_b so that the coefficients of the operators are determined by high momentum physics, where the light quarks can be treated using perturbation theory.

In the minimal Standard Model a complete set of operators that have the right flavor quantum numbers to contribute are six four–quark operators and the two–quark operators

$$Q_1 = \bar{s}_L \not{D} D_\mu D^\mu b_L \quad , \tag{2.6a}$$

$$Q_2 = \bar{s}_L D_\mu \not{D} D^\mu b_L - 1/2\ \bar{s}_L D_\mu D^\mu \not{D} b_L \quad , \tag{2.6b}$$

$$Q_3 = \bar{s}_L D_\mu \not{D} D^\mu b_L \quad , \tag{2.6c}$$

$$Q_4 = \bar{s}_L \not{D}\not{D}\not{D} b_L \quad , \tag{2.6d}$$

$$Q_5 = g \bar{s}_L T^a \gamma^\mu b_L D^\nu G^a_{\mu\nu} \quad , \tag{2.6e}$$

$$Q_6 = g G^a_{\mu\nu} \bar{s}_L T^a \gamma^\mu D^\nu b_L \quad , \tag{2.6f}$$

$$Q_7 \;=\; g\tilde{G}^a_{\mu\nu}\bar{s}_L T^a \gamma^\mu D^\nu b_L \quad , \tag{2.6g}$$

$$Q_8 \;=\; e m_b \bar{s}_L \sigma^{\mu\nu} b_R F_{\mu\nu} \quad , \tag{2.6h}$$

$$Q_9 \;=\; g m_b \bar{s}_L \sigma^{\mu\nu} T^a b_R G^a_{\mu\nu} \quad , \tag{2.6i}$$

$$Q_{10} \;=\; m_b \bar{s}_L \not{D}\not{D} b_R \quad . \tag{2.6j}$$

In eqs. (2.6) $G^a_{\mu\nu}$ is the field strength tensor for the strong interactions, $\tilde{G}^a_{\mu\nu}$ is its dual, $F_{\mu\nu}$ is the electromagnetic field strength tensor and the covariant derivative is

$$D_\mu \;\equiv\; \partial_\mu \;+\; igT^a A^a_\mu \;+\; ieQ_b A_\mu \quad . \tag{2.7}$$

We work to first order in the electromagnetic interactions.

Since the effective Hamiltonian is ultimately to be used to compute S–matrix elements, the equations of motion can be used [2.5] to reduce the operator basis (2.6) to four–quark operators and the magnetic moment type operators Q_8 and Q_9. Operators Q_1, Q_4, and Q_{10} vanish by the equations of motion (e.g., $\not{D} s_L = 0$, neglecting the strange quark mass). Operator Q_5 is equivalent to a four–quark operator. For Q_3 first note that

$$\begin{aligned}\bar{s}_L D^\mu \not{D} D_\mu b_L &= \bar{s}_L [D^\mu, D^\nu]\gamma_\nu D_\mu b_L \\ &= ig\bar{s}_L T^a G^a_{\mu\nu}\gamma^\nu D^\mu b_L \;+\; iQ_b e \bar{s}_L F_{\mu\nu}\gamma^\nu D^\mu b_L \quad .\end{aligned} \tag{2.8}$$

Next note that

$$\begin{aligned}F^{\mu\nu}\bar{s}_L \gamma^\nu D^\mu b_L &= (1/2)\; F_{\mu\nu}\bar{s}_L\gamma^\nu\{\gamma^\mu, \not{D}\} b_L \\ &= -(1/2)\; m_b F_{\mu\nu}\bar{s}_L \sigma^{\nu\mu} b_R \;+\; (1/2)\; F_{\mu\nu}\bar{s}_L\{\gamma^\nu, \not{D}\}\gamma^\mu b_L \, ,\end{aligned} \tag{2.9}$$

which yields

$$F_{\mu\nu}\bar{s}_L\gamma^\nu D^\mu b_L \;=\; (1/4)\; m_b \bar{s}_L \sigma^{\mu\nu} b_R F_{\mu\nu} \quad . \tag{2.10}$$

A similar manipulation for $\bar{s}_L G_{\mu\nu}\gamma^\nu D^\mu b_L$ gives (with $G_{\mu\nu} = G^a_{\mu\nu}T^a$)

$$\bar{s}_L G_{\mu\nu}\gamma^\nu D^\mu b_L \;=\; (1/4)\; m_b \bar{s}_L \sigma^{\mu\nu} G_{\mu\nu} b_R \;+\; (\text{four}-\text{quark operators})\,, \qquad (2.11)$$

implying that Q_6 is equivalent to Q_9 plus four–quark operators. Combining eqs. (2.8), (2.10), and (2.11) gives

$$Q_3 \;=\; \frac{iQ_b e}{4} Q_8 \;+\; \frac{ig}{4} Q_9 \;+\; (\text{four}-\text{quark operators}) \quad . \qquad (2.12)$$

For Q_7, use the gamma matrix identity, $\gamma_\nu\gamma_\lambda\gamma_\sigma = \eta_{\nu\lambda}\gamma_\sigma + \eta_{\lambda\sigma}\gamma_\nu - \eta_{\sigma\nu}\gamma_\lambda - i\gamma_5\gamma^\mu\epsilon_{\mu\nu\lambda\sigma}$, to deduce that

$$\begin{aligned}\bar{s}_L \tilde{G}_{\mu\nu}\gamma^\mu D^\nu b_L &= i\left[\bar{s}_L \not{D}\gamma^\lambda\gamma^\sigma G_{\lambda\sigma} b_L - 2\bar{s}_L \gamma^\sigma D^\lambda G_{\lambda\sigma} b_L\right] \\ &= 2i\bar{s}_L G_{\lambda\sigma}\gamma^\lambda D^\sigma b_L \;+\; (\text{four}-\text{quark operators}) \quad ,\end{aligned}$$

so Q_7 is equivalent to Q_6 plus four–quark operators.

For Q_2 we note that

$$\begin{aligned}\bar{s}_L D_\mu D^\mu \not{D} b_L = \; -im_b \bar{s}_L D^\mu D_\mu b_R \;&=\; \frac{im_b}{2}\bar{s}_L[\gamma^\mu,\gamma^\nu]D_\mu D_\nu b_R \\ =\; \frac{m_b}{2}\,\bar{s}_L\,\sigma^{\mu\nu}[igG_{\mu\nu} \;&+\; ieQ_b F_{\mu\nu}]b_R \quad .\end{aligned} \qquad (2.13)$$

Eqs. (2.12) and (2.13) imply that Q_2 is equivalent to four–quark operators; it has no magnetic moment piece.

An operator basis for the effective Hamiltonian for weak radiative $\bar{B}$–meson decay thus consists of four–quark operators and the magnetic moment–type operators. We write (to leading order in small weak mixing angles) the effective Hamiltonian density as

$$\mathcal{H}_{\text{eff}} = \left(4G_F/\sqrt{2}\right)\left(s_3 + s_2 e^{i\delta}\right) \sum_{j=1}^{8} C_j(\mu) O_j(\mu) \quad , \tag{2.14}$$

where (displaying the color indices explicitly)

$$O_1 = (\bar{c}_{L\beta}\gamma^\mu b_{L\alpha})(\bar{s}_{L\alpha}\gamma_\mu c_{L\beta}) \quad , \tag{2.15a}$$

$$O_2 = (\bar{c}_{L\alpha}\gamma^\mu b_{L\alpha})(\bar{s}_{L\beta}\gamma_\mu c_{L\beta}) \quad , \tag{2.15b}$$

$$O_3 = (\bar{s}_{L\alpha}\gamma^\mu b_{L\alpha})\Big[(\bar{u}_{L\beta}\gamma_\mu u_{L\beta}) + \ldots + (\bar{b}_{L\beta}\gamma_\mu b_{L\beta})\Big] \quad , \tag{2.15c}$$

$$O_4 = (\bar{s}_{L\alpha}\gamma^\mu b_{L\beta})\Big[(\bar{u}_{L\beta}\gamma_\mu u_{L\alpha}) + \ldots + (\bar{b}_{L\beta}\gamma_\mu b_{L\alpha})\Big] \quad , \tag{2.15d}$$

$$O_5 = (\bar{s}_{L\alpha}\gamma^\mu b_{L\alpha})\Big[(\bar{u}_{R\beta}\gamma_\mu u_{R\beta}) + \ldots + (\bar{b}_{R\beta}\gamma_\mu b_{R\beta})\Big] \quad , \tag{2.15e}$$

$$O_6 = (\bar{s}_{L\alpha}\gamma^\mu b_{L\beta})\Big[(\bar{u}_{R\beta}\gamma_\mu u_{R\alpha}) + \ldots + (\bar{b}_{R\beta}\gamma_\mu b_{R\alpha})\Big] \quad , \tag{2.15f}$$

$$O_7 = (e/16\pi^2) m_b \bar{s}_{L\alpha}\sigma^{\mu\nu} b_{R\alpha} F_{\mu\nu} \quad , \tag{2.15g}$$

$$O_8 = (g/16\pi^2) m_b \bar{s}_{L\alpha}\sigma^{\mu\nu} T^a_{\alpha\beta} b_{R\beta} G^a_{\mu\nu} \quad . \tag{2.15h}$$

We shall integrate out the top quark and W–boson together. This approximation amounts to neglecting the running of the strong interaction fine structure constant between m_t and M_W (compared with how much it runs between M_W and m_b). Since the strong coupling constant varies little over the range between 50 and 150 GeV, where the top quark is expected to be found, the strong coupling constant at the top and at the W scales should be the same within ten percent. The coefficients $C_j(M_W)$ are determined solely by high momentum physics and can be computed using perturbation theory. With $\mu = M_W$ the large logarithms are in the matrix elements of the operators $O_1 - O_8$. These large logarithms are transferred from the matrix elements of the operators to their coefficients C_j by scaling the subtraction point μ down from M_W to m_b using the renormalization group equations

$$\mu \frac{d}{d\mu} C_j(\mu) - \sum_{i=1}^{8} \gamma_{ij}(g) C_i(\mu) = 0 \quad , \tag{2.16}$$

which follow from the μ–independence of the effective Hamiltonian density in eq. (2.14). Here γ is the anomalous dimension matrix for the operator basis in eqs. (2.15). It takes into account the subtraction point dependence of the renormalized operators.

We use dimensional regularization with minimal subtraction to define the operators [2.6]. Recall that in n–dimensions the quark fields have dimension $(n-1)/2$, the gauge fields have dimension $(n-2)/2$, and the bare gauge couplings have dimension $(4-n)/2$. The renormalized gauge couplings are, however, dimensionless. It follows that the bare operators $O_j^{(0)}, j = 1, \ldots, 6$ and the renormalized operators $O_j, j = 1, \ldots, 6$ have dimension $2n-2$. On the other hand the bare operators $O_7^{(0)}$ and $O_8^{(0)}$ have dimension $n+2$ while the renormalized operators O_7 and O_8 have dimension $3n/2$.

The bare, μ–independent, operators $O_j^{(0)}$ are related to the renormalized ones via

$$O_j(\mu) = \sum_{i=1}^{8} \mu^{\epsilon D_j} Z_{ji} \, \mu^{-\epsilon D_i^{(0)}} O_i^{(0)} \quad , \tag{2.17}$$

where Z_{ji} is dimensionless and has a perturbative expansion of the form

$$Z_{ij} = \delta_{ij} + \frac{g^2}{8\pi^2 \epsilon} Z_{ij}^{(1)} + \ldots \quad , \tag{2.18}$$

and

$$\epsilon D_j = \text{dimension}[O_j] - (2n-2) \quad , \tag{2.19a}$$

$$\epsilon D_j^{(0)} = \text{dimension}[O_j^{(0)}] \; - \; (2n-2) \quad . \tag{2.19b}$$

Here

$$n \; = \; 4 \; - \; \epsilon \quad . \tag{2.20}$$

Using the subtraction point dependence of the strong gauge coupling g

$$\mu \frac{dg}{d\mu} \; = \; -\frac{\epsilon g}{2} \; + \; \beta(g) \quad , \tag{2.21}$$

it follows that $\gamma_{ij}(g)$ has the perturbative expansion

$$\gamma_{ij}(g) \; = \; -\frac{g^2}{8\pi^2} \, Z_{ij}^{(1)}(1 + D_j^{(0)} - D_i^{(0)}) + \ldots \quad . \tag{2.22}$$

The dimensions of the renormalized operators do not affect the anomalous dimensions; γ_{ij} only depends on the dimensions of the bare operators, $D_j^{(0)}$. Explicitly

$$D_i^{(0)} \; = \; \begin{cases} 0 & i = 1, \ldots, 6 \\ 1 & i = 7, 8 \quad . \end{cases} \tag{2.23}$$

The solution to the renormalization group eqs. (2.16) is (using a somewhat schematic matrix notation)

$$C(\mu) \; = \; \left[\exp \int\limits_{g(M_W)}^{g(\mu)} dg \; \frac{\gamma^T(g)}{\beta(g)} \right] C(M_W) \quad . \tag{2.24}$$

To get the coefficients $C_j(m_b)$, the matching conditions $C_j(M_W)$ are required. In the leading logarithmic approximation, the matching conditions for the four–quark operators O_1–O_6 are determined by the tree level W–boson exchange. This gives

$$C_2(M_W) = 1 \quad , \tag{2.25a}$$

$$C_j(M_W) = 0 \quad j = 1,3,4,5,6 \quad . \tag{2.25b}$$

The one–loop mixing under renormalization of the four–quark operators O_1–O_6 with the magnetic moment type operator O_7 (and O_8) vanishes. Therefore, in the leading logarithmic approximation, the value of $C_7(M_W)$ in the minimal Standard Model follows from the one–loop Feynman diagrams in Fig. 3. They give [2.7]

$$C_7(M_W) \;=\; -\frac{1}{2}\,A(x) \quad , \tag{2.26}$$

where

$$A(x) = x\left[\frac{2/3x^2 + 5/12x - 7/12}{(x-1)^3} - \frac{(3/2x^2 - x)\ell n x}{(x-1)^4}\right] \quad , \tag{2.27}$$

with

$$x \;=\; m_t^2/M_W^2 \quad . \tag{2.28}$$

(Note that if the one–loop mixing of operators O_1–O_6 with O_7 had not vanished then, in the leading logarithmic approximation, it would have been appropriate to set $C_7(M_W) = 0$.) Fig. 4 shows a plot of the function $A(x)$.

In the leading logarithmic approximation, the value of $C_8(M_W)$ in the minimal Standard Model is determined by the one–loop diagrams in Fig. 5. They give [2.8]

$$C_8(M_W) \;=\; -\frac{1}{2}\,D(x) \quad , \tag{2.32}$$

where

$$D(x) \;=\; \frac{x}{2}\left(\frac{1/2x^2 - 5/2x - 1}{(x-1)^3} + \frac{3x\ell n x}{(x-1)^4}\right) \quad . \tag{2.33}$$

Fig. 6 shows a plot of $D(x)$.

To determine the matching conditions $C_7(M_W)$ and $C_8(M_W)$, we used the operator basis (2.15) that was reduced using the equations of motion. On–shell $b \to s\gamma$ and $b \to sg$ matrix elements of O_7 and O_8 were compared with the on–shell calculation of the $b \to s\gamma$ and $b \to sg$ matrix elements in the minimal Standard Model. (The on–shell one–loop $b \to s\gamma$ and $b \to sg$ matrix elements of O_1–O_6 vanish.) It is also possible to work off–shell, matching one particle irreducible Green's functions in the models we consider with one particle irreducible Green's functions in our effective field theory.

References for Chapter 2

2.1 F. Gilman and M. Wise, Phys. Rev. **D20**, 2392 (1979); E. Witten, Nucl. Phys. **B104** (1976) 445; E. Witten, Nucl. Phys. **B122** (1977) 109; M. A. Shifman et al., Nucl. Phys. **B120** (1977) 316.

2.2. S.L. Glashow, Nucl. Phys. **22** (1961) 579; S. Weinberg, Phys. Rev. Lett. **19** (1967) 1264; A. Salam, in *Elementary Particle Physics: Relativistic Groups and Analyticity*, Nobel Symp. No. 8, ed. N. Svartholm (Almqvist and Wiksell, Stockholm, 1968), p. 367.

2.3. M. Kobayashi and T. Maskawa, Prog. Theor. Phys. **49** (1973) 652.

2.4. G. Yost *et al.* (Particle Data Group), Phys. Lett. **B204** (1988) 1.

2.5. H.D. Politzer, Nucl. Phys. **B172** (1980) 349.

2.6. G. 'tHooft, Nucl. Phys. **B61** (1973) 455.

2.7. T. Inami and C.S. Lim, Prog. Theor. Phys. **65** (1981) 297.

2.8. R. Grigjanis, P.J. Odonnell, M. Sutherland and H. Navelet, Phys. Lett. **B213** (1988) 355.

Chapter 3. The Anomalous Dimension Matrix

The values of the coefficients $C_j(\mu)$, at a subtraction point $\mu << M_W$, are given somewhat schematically by equation (2.24). They depend on the matching conditions $C_i(M_W)$, which were calculated in the previous section (for the minimal Standard Model) and on the 8×8 anomalous dimension matrix γ_{ij}. In this section, we compute the anomalous dimension matrix and explicitly solve the renormalization group equations.

The one–loop mixing of the operators $O_1, \ldots, O_6$ has been studied previously [3.1]. The magnetic moment type operators O_7 and O_8 do not mix with O_1–O_6 since, if the factor of m_b is removed, they are only dimension five. Their self–renormalization has been determined to give [3.2]

$$\gamma_{77} = \frac{16}{3}\frac{g^2}{8\pi^2} \quad , \quad \gamma_{88} = \frac{14}{3}\frac{g^2}{8\pi^2} \quad . \tag{3.1}$$

Eq. (3.1) includes the μ–dependence that arises from the running b–quark mass in O_7 and O_8 and the strong coupling in O_8. The operator O_8 mixes with O_7 at one–loop† yielding [3.4]

$$\gamma_{87} = -\frac{16}{9}\frac{g^2}{8\pi^2} \quad . \tag{3.2}$$

Since we work only to first order in electromagnetic interactions, O_7 does not mix with O_8 so

$$\gamma_{78} = 0 \quad . \tag{3.3}$$

The mixing of $O_1, \ldots, O_6$ with O_7 and O_8 first occurs at two–loops. Despite this it

† In our original work [3.3] we incorrectly concluded that this mixing vanishes. This error, however, has (as we shall see in Chapter IV) a small impact on $C_7(m_b)$ in the Standard Model with a minimal Higgs sector.

must be included in order to determine $C_7(\mu)$ and $C_8(\mu)$ in the leading logarithmic approximation. Recall that the matching conditions for the magnetic moment–type operators, $C_7(M_W)$ and $C_8(M_W)$, are a one–loop effect and their scaling through the renormalization of O_7 and O_8 is also a one loop effect. On the other hand for O_1–O_6, the matching conditions $C_1(M_W)$–$C_6(M_W)$ are a tree level effect, while the mixing of these operators with O_7 and O_8 is a two–loop effect. By including the factors $e/16\pi^2$ and $g/16\pi^2$ in the definitions of O_7 and O_8, all the matching conditions $C_i(M_W), i = 1, \ldots, 8$ (see eqs. (2.25) and (2.26)) are order unity and the elements of the anomalous dimension matrix $\gamma_{ij}, i, j = 1, \ldots, 8$ are all order $g^2/8\pi^2$.

The tracelessness of the generators T^a of SU(3) color implies that the two–loop mixing of O_1 with O_7 vanishes. Thus γ has the form (the X_i and Y_i are unknown operator mixing elements at this point):

$$\gamma = \frac{g^2}{8\pi^2}\begin{pmatrix} -1 & 3 & 0 & 0 & 0 & 0 & 0 & Y_1 \\ 3 & -1 & -1/9 & 1/3 & -1/9 & 1/3 & X_2 & Y_2 \\ 0 & 0 & -11/9 & 11/3 & -2/9 & 2/3 & X_3 & Y_3 \\ 0 & 0 & 22/9 & 2/3 & -5/9 & 5/3 & X_4 & Y_4 \\ 0 & 0 & 0 & 0 & 1 & -3 & X_5 & Y_5 \\ 0 & 0 & -5/9 & 5/3 & -5/9 & -19/3 & X_6 & Y_6 \\ 0 & 0 & 0 & 0 & 0 & 0 & 16/3 & 0 \\ 0 & 0 & 0 & 0 & 0 & 0 & -16/9 & 14/3 \end{pmatrix} . \quad (3.4)$$

With the subtraction point, $\mu = m_b$, there are no large logarithms in the matrix elements of O_1–O_8 responsible for $\bar{B}$–meson decay. The on–shell $b \to s\gamma$ matrix elements of O_1–O_6 vanish at one loop. Therefore when the inclusive rate for $\bar{B} \to X_s\gamma$ (with E_γ large) is modelled by b–quark decay, it is determined, in the leading logarithmic approximation, by the tree–level matrix element of $O_7(m_b)$:

$$\Gamma(\bar{B} \to X_s\gamma) = (s_2^2 + s_3^2 + 2s_2s_3c_\delta) \frac{G_F^2 m_b^5 \alpha_{em}}{32\pi^4} |C_7(m_b)|^2 \quad . \tag{3.5}$$

(Note that if the on–shell one–loop $b \to s\gamma$ matrix elements of O_1–O_6 had not vanished then these matrix elements would have made a contribution comparable to the tree level matrix element of O_7.) In eq. (3.5) α_{em} is the electromagnetic fine structure constant, $\alpha_{em} = e^2/4\pi$.

A simple analytic formula for $C_7(m_b)$ can be derived by truncating the anomalous dimension matrix. If the mixing of O_2 with the other four quark operators and with the gluon magnetic moment operator is neglected, then eq. (2.24) yields, for $\mu << M_W$,

$$\begin{aligned} C_7(\mu) = \left[\frac{\alpha_s(M_W)}{\alpha_s(\mu)}\right]^{16/23} \Bigg\{ C_7(M_W) - \frac{8}{3} C_8(M_W)\left[1 - \left(\frac{\alpha_s(\mu)}{\alpha_s(M_W)}\right)^{2/23}\right] \\ + \frac{3X_2}{19}\left[1 - \left(\frac{\alpha_s(\mu)}{\alpha_s(M_W)}\right)^{19/23}\right]\Bigg\} . \end{aligned} \tag{3.6}$$

Here we used [3.5]

$$\beta(g) = -(11 - 2/3N_f) \frac{g^3}{16\pi^2} \quad , \tag{3.7}$$

with $N_f = 5$ (appropriate to an effective five quark theory). In eq. (3.6) α_s is the strong interaction fine structure constant $\alpha_s = g^2/4\pi$.

This truncation of the anomalous dimension matrix is an additional approximation beyond the leading logarithmic approximation. While it correctly gives the $[\alpha_s(\mu)/\pi]\ell n(m_t^2/\mu^2)$ term in the perturbative expansion of $C_7(\mu)$, some contributions to the $\{[\alpha_s(\mu)/\pi]\ell n(m_t^2/\mu^2)\}^p$ terms are missing for $p \geq 2$. As will be discussed in Chapter 4, we expect that (in the minimal Standard Model) the errors induced in

$C_7(m_b)$ by this truncation are less than 15%. The remainder of this section is devoted to the computation of X_2.

We define our operators using dimensional regularization with minimal subtraction. Dimensional regularization, however, is plagued with difficulties in nonvector–like–theories. These stem from the inability to extend the Dirac matrix γ_5 and the totally antisymmetric symbol $\epsilon_{\mu\nu\lambda\sigma}$ to n–dimensions. Because the mixing of O_2 with O_7 is a two–loop effect, it is important in the calculation of X_2 to handle the γ_5s, which occur in the definitions of O_2 and O_7, correctly. As a step in that direction we prove that if the magnetic moment counterterm to O_2 is ZO_7, then $Z\hat{O}_7$, where

$$\hat{O}_7 \;=\; \frac{e}{16\pi^2}\, m_b\, \bar{s}_\alpha\, \sigma_{\mu\nu}\, b_\alpha\, F^{\mu\nu} \quad , \tag{3.8}$$

is the magnetic moment counterterm to the vector operator

$$\hat{O}_2 \;=\; (\bar{s}_\alpha \gamma^\mu c_\alpha)(\bar{c}_\beta \gamma_\mu b_\beta) \quad . \tag{3.9}$$

First note that the parity invariance of the strong interactions implies that the operator

$$\tilde{O}_2 \;=\; (\bar{s}_{R\alpha} \gamma^\mu c_{R\alpha})(\bar{c}_{R\beta} \gamma_\mu b_{R\beta}) \quad , \tag{3.10}$$

has the magnetic moment type counterterm $Z\tilde{O}_7$ where

$$\tilde{O}_7 \;=\; \frac{e}{16\pi^2}\, m_b\, (\bar{s}_{R\alpha}\, \sigma_{\mu\nu} b_{L\alpha}) F^{\mu\nu} \quad , \tag{3.11}$$

is the parity transform of O_7. So the parity even operator

$$O_2 + \tilde{O}_2 = \frac{1}{2}(\bar{s}_\alpha \gamma^\mu c_\alpha)(\bar{c}_\beta \gamma_\mu b_\beta) + \frac{1}{2}(\bar{s}_\alpha \gamma^\mu \gamma_5 c_\alpha)(\bar{c}_\beta \gamma_\mu \gamma_5 b_\beta) \quad , \tag{3.12}$$

has the magnetic moment counterterm $Z\hat{O}_7$. Since the parity even operators $\frac{1}{2}(\bar{s}_\alpha \gamma^\mu c_\alpha)(\bar{c}_\beta \gamma_\mu b_\beta)$ and $\frac{1}{2}(\bar{s}_\alpha \gamma^\mu \gamma_5 c_\alpha)(\bar{c}_\beta \gamma_\mu \gamma_5 b_\beta)$ are related by the non–anomalous discrete chiral symmetry $c_\alpha \to \gamma_5 c_\alpha, u_\alpha \to \gamma_5 u_\alpha$, they both have the same magnetic moment counterterm $\frac{1}{2} Z \hat{O}_7$. This completes the demonstration that the magnetic moment counterterm to the vector operator $\hat{O}_2$ is $Z\hat{O}_7$ if and only if the magnetic moment counterterm to O_2 is ZO_7. This relationship holds in any renormalization scheme that preserves the parity and discrete chiral symmetries of QCD. Furthermore, in the leading logarithmic approximation, γ_{27} (which follows from Z) is a physical quantity and must have the same value in any (acceptable) renormalization scheme. Dimensional regularization with minimal subtraction can be used to compute the magnetic moment counterterm $Z\hat{O}_7$ to the vector operator $\hat{O}_2$ since γ_5 never appears in this calculation and no Fiertz identities are used. This prescription for Z is equivalent to having γ_5 anticommuting in the calculation of the two–loop mixing of O_2 into O_7 (i.e., to following the chirality of the quark lines through the graphs). Since the products of γ–matrices can be reduced using n–dimensional gamma matrix identities that don't involve $\epsilon_{\mu\nu\lambda\sigma}$, and no trace over gamma matrices is taken, treating γ_5 as anticommuting makes the calculation of the mixing of O_2 with O_7 manifestly identical to the calculation of the mixing of $\hat{O}_2$ with $\hat{O}_7$.

To compute the mixing of O_2 with O_7 we work off–shell. Therefore the mixing of O_2 with the complete off–shell basis Q_1–Q_{10} is considered and then the equations of motion are used to reduce this basis. While it is possible to work on–shell to compute the anomalous dimension matrix element γ_{27}, working off–shell offers two major advantages:

(*i*) Only one–particle–irreducible (1PI) Green's functions need be considered so there are less Feynman diagrams to compute than there would be working on–shell.

(*ii*) Of the operators Q_1–Q_7 only Q_3 is relevant; the others have no (electromagnetic) magnetic moment piece when the equations of motion are applied. Similarly, of the operators Q_8–Q_{10}, only Q_8 is relevant. It is possible to pick out the mixing of O_2 with Q_3, and O_2 with Q_8 by focussing on one particular Lorentz structure so that it is not necessary to compute the complete off–shell 1PI Green's functions. This makes the calculations less tedious than if we had worked on–shell.

The amputated 1PI tree level $b(p) \to s(p')\gamma(k)$ Green's functions of the operators $Q_i, i = 1, \ldots, 7$, inserted at zero momentum (so that $p' = p - k$), can be written as

$$\Big[\alpha_i^{(1)} \not\epsilon \not p \not k + \alpha_i^{(2)} \not\epsilon p \cdot k + \alpha_i^{(3)} \not\epsilon p^2 + \alpha_i^{(4)} \not\epsilon k^2 + \alpha_i^{(5)} \not p \epsilon \cdot k + \alpha_i^{(6)} \not p \epsilon \cdot p + \alpha_i^{(7)} \not k \epsilon \cdot p + \alpha_i^{(8)} \not k \epsilon \cdot k\Big] \frac{(1-\gamma_5)}{2} \quad . \tag{3.13}$$

Here ϵ^μ is the polarization vector for the electromagnetic field A^μ. Since the Green's function is off–shell, the condition $\epsilon \cdot k = 0$ is not imposed. The crucial observation is that $\alpha_i^{(2)}$ vanishes unless $i = 3$ and for that case $\alpha_3^{(2)} = iQ_b e$. Thus to isolate the mixing of O_2 with Q_3 it suffices to extract the piece of the $b(p) \to s(p-k)\gamma(k)$ Green's function with Lorentz structure $\not\epsilon p \cdot k$.

A simple application of this result is that the potential one–loop mixing of Fig. 7 vanishes. In Fig. 7 the loop integral can only produce a term quadratic in k (i.e., $\not\epsilon k^2$ or $\not k \epsilon \cdot k$). Similarly, the two–loop graphs in Fig. 8 can also be shown to be irrelevant.

The amputated 1PI tree level $b(p) \to s(p')\gamma(k)$ Green's functions of the operators $Q_i, i = 8, 9, 10$ inserted at zero momentum (so that $p' = p - k$), can be written as

$$m_b \Big[\beta_i^{(1)} \not k \not\epsilon + \beta_i^{(2)} \not\epsilon \not k + \beta_i^{(3)} \not p \not\epsilon + \beta_i^{(4)} \not\epsilon \not p\Big] \frac{(1+\gamma_5)}{2} \quad . \tag{3.14}$$

The coefficient of $\beta_i^{(2)}$ vanishes unless $i = 8$ and in that case $\beta_8^{(2)} = e$. Therefore the mixing of O_2 with Q_8 can be isolated by extracting the piece of the $b(p) \to s(p-k)\gamma(k)$ Green's function with Lorentz structure $\not{\epsilon}\not{k}$.

In summary, the mixing of O_2 with Q_3 and Q_8 can be derived from the two–loop Feynman diagrams in Figs. 9–15 by extracting the $\not{\epsilon} p \cdot k$ and $\not{\epsilon}\not{k}$ Lorentz structures, respectively (when other Lorentz structures are expressed in the basis of eqs. (3.13) and (3.14)). Moreover, by treating insertions of the b–quark mass (which flip chirality) perturbatively, graphs without an insertion shown in Figs. 9–12 contribute only to the mixing with Q_3 while those with a mass insertion (Figs. 13–15, denoted by a cross) contribute only to the mixing with Q_8.

The calculation of X_2 is further simplified by noting that the graphs in each pair of Figs. 9–11 are related by charge conjugation. Consider the graphs in Fig. 9. In Feynman gauge they give

$$\frac{4}{3}\, eg^2 Q_c \Big[J^{(1)}(p', k) + J^{(2)}(p, k) \Big] \frac{(1-\gamma_5)}{2} \quad . \tag{3.15}$$

Here $Q_c = 2/3$ is the charge of the charm quark, the identity $T^a_{\alpha\beta} T^a_{\beta\gamma} = (4/3)\delta_{\alpha\gamma}$ has been used, and $J^{(1)}$ and $J^{(2)}$, which correspond respectively to Figs. (9a) and (9b), are given by

$$J^{(1)}(p', k) = \int \frac{d^n q}{(2\pi)^n} \int \frac{d^n r}{(2\pi)^n}\, \gamma^\mu \, \frac{1}{\not{r} + \not{p}'}\, \gamma^\lambda \, \frac{1}{\not{q} + \not{r}}\, \gamma_\mu \frac{1}{\not{q}}\, \not{\epsilon}\, \frac{1}{\not{q} + \not{k}}\, \gamma_\lambda \, \frac{1}{r^2} \; , \tag{3.16}$$

and

$$J^{(2)}(p, k) = \int \frac{d^n q}{(2\pi)^n} \int \frac{d^n r}{(2\pi)^n}\, \gamma^\lambda \, \frac{1}{\not{q} - \not{k}}\, \not{\epsilon}\, \frac{1}{\not{q}}\, \gamma^\mu \frac{1}{\not{q} + \not{r}}\, \gamma_\lambda \, \frac{1}{\not{r} + \not{p}}\, \gamma_\mu \, \frac{1}{r^2} \quad . \tag{3.17}$$

Let C be the charge conjugation matrix

$$C\, \gamma^\mu\, C^{-1} = -\gamma^{\mu T} \quad , \tag{3.18}$$

(where the superscript T denotes the transpose). From eqs. (3.16)–(3.18) it follows that,

$$J^{(2)}(p,k) \;=\; -C^{-1}[J^{(1)}(p,-k)]^T\, C \quad . \tag{3.19}$$

Thus $J^{(2)}$ may be extracted from the computation of $J^{(1)}$. In the computation of $J^{(1)}$ we keep p' arbitrary and expand to linear order in powers of k. Keeping p' arbitrary regulates possible infrared divergences and higher powers of k are not necessary since we are only after the part of $J^{(1)} + J^{(2)}$ that goes as $\not{\epsilon}p\cdot k$.

Writing (to linear order in k)

$$J^{(1)}(p',k) = \alpha(p'^2)\not{\epsilon}p'\cdot k + \beta(p'^2)\not{\epsilon}\not{p}'\not{k} + \gamma(p'^2)\not{\epsilon}p'^2 \quad , \tag{3.20}$$

then eq. (3.19) gives

$$J^{(2)}(p,k) = -\alpha(p^2)\not{\epsilon}p\cdot k \; - 2\beta(p^2)\not{\epsilon}p\cdot k + \beta(p^2)\not{\epsilon}\not{p}\not{k} \; + \ldots, \tag{3.21}$$

and so

$$\begin{aligned} J^{(1)} + J^{(2)} &= \not{\epsilon}p\cdot k[\alpha(p'^2) - \alpha(p^2) - 2\beta(p^2) - 2\gamma(p'^2)] \\ &\quad + \big(\beta(p^2) + \beta(p'^2)\big)\not{\epsilon}\not{p}\not{k} + \gamma(p'^2)\not{\epsilon}p^2 \; + \ldots \quad . \end{aligned} \tag{3.22}$$

Dimensional analysis in $n = 4 - \epsilon$ dimensions implies that

$$\alpha(p^2) \;=\; \frac{\alpha_0}{(-p^2)^\epsilon} \quad , \quad \beta(p^2) \;=\; \frac{\beta_0}{(-p^2)^\epsilon} \quad , \quad \gamma(p^2) \;=\; \frac{\gamma_0}{(-p^2)^\epsilon} \quad . \tag{3.23}$$

Using (3.23) and the expansion

$$\gamma(p'^2) = \gamma(p^2)\Big(1 + 2\,\epsilon\frac{p\cdot k}{p^2} + O(\epsilon^2)\Big) \quad , \tag{3.24}$$

we finally arrive at

$$J^{(1)} + J^{(2)} = \frac{1}{(-p^2)^\epsilon} \not{\epsilon} p \cdot k[-2\beta_0 - 2(1-\epsilon)\gamma_0] + \ldots, \tag{3.25}$$

where the ellipses stand for terms that correspond to the other possible invariants. So to extract the coefficient of $\not{\epsilon} p \cdot k$ in $J^{(1)} + J^{(2)}$ we need only compute the coefficients of $\not{\epsilon}\not{p}'\not{k}$ and $\not{\epsilon} p'^2$ in $J^{(1)}$.

It is straightforward to compute $J^{(1)}$. For book-keeping purposes it is useful to do the integrals and γ–matrix algebra separately. We write

$$J^{(1)} = J^{(1)}_{\alpha\beta\gamma\delta}\, T^{(1)\alpha\beta\gamma\delta} \quad , \tag{3.26}$$

where

$$T^{(1)\alpha\beta\gamma\delta} \equiv \gamma^\mu\gamma^\alpha\gamma^\lambda\gamma^\beta\gamma_\mu\gamma^\gamma\not{\epsilon}\gamma^\delta\gamma_\lambda \quad . \tag{3.27}$$

Expanding to linear order in k gives

$$J^{(1)}_{\alpha\beta\gamma\delta} = -2k^\rho\, K^{(1a)}_{\alpha\beta\gamma\delta\rho} + k_\delta K^{(1b)}_{\alpha\beta\gamma} + K^{(1c)}_{\alpha\beta\gamma\delta} \quad , \tag{3.28}$$

where

$$K^{(1a)}_{\alpha\beta\gamma\delta\rho} = \int \frac{d^n r}{(2\pi)^n} \int \frac{d^n q}{(2\pi)^n} \frac{(r+p')_\alpha (q+r)_\beta q_\gamma q_\delta q_\rho}{r^2(r+p')^2(q+r)^2(q^2)^3} \quad , \tag{3.29a}$$

$$K^{(1b)}_{\alpha\beta\gamma} = \int \frac{d^n r}{(2\pi)^n} \int \frac{d^n q}{(2\pi)^n} \frac{(r+p')_\alpha (q+r)_\beta q_\gamma}{r^2(r+p')^2(q+r)^2(q^2)^2} \quad , \tag{3.29b}$$

$$K^{(1c)}_{\alpha\beta\gamma\delta} = \int \frac{d^n r}{(2\pi)^n} \int \frac{d^n q}{(2\pi)^n} \frac{(r+p')_\alpha (q+r)_\beta q_\gamma q_\delta}{r^2(r+p')^2(q+r)^2(q^2)^2} \quad . \tag{3.29c}$$

The divergent parts of these integrals are straightforward to compute. For example

$$K^{(1b)}_{\alpha\beta\gamma} = -\frac{1}{(16\pi^2)^{n/2}}\,(-p'^2)^{-\epsilon}\Gamma(1+\epsilon)\Bigg[\left(\frac{1}{4\epsilon^2}+\frac{29}{48\epsilon}\right)p'_\alpha\eta_{\beta\gamma} + \frac{1}{24\epsilon}(p'_\beta\eta_{\alpha\gamma}+p'_\gamma\eta_{\alpha\beta})\Bigg] \quad . \tag{3.30}$$

Similar expressions for $K^{(1a)}$ and $K^{(1c)}$ can be found in the appendix. The results can then be contracted into $T^{(1)\alpha\beta\gamma\delta}$ and reduced using n–dimensional γ–matrix algebra. For example, for $k_\delta K^{(1b)}_{\alpha\beta\gamma}T^{(1)\alpha\beta\gamma\delta}$ we need to compute the contractions of $k_\delta p'_\alpha\eta_{\beta\gamma}$, $k_\delta p'_\beta\eta_{\alpha\gamma}$, and $k_\delta p'_\gamma\eta_{\alpha\beta}$ with $T^{(1)\alpha\beta\gamma\delta}$ and extract the coefficients of $\not\epsilon\not p'\not k$. These are $8-4\epsilon$, -12ϵ, and $-8+4\epsilon$ respectively. Thus

$$k_\delta K^{(1b)}_{\alpha\beta\gamma}T^{(1)\alpha\beta\gamma\delta} \;=\; -\frac{1}{(16\pi^2)^{n/2}}\,(-p'^2)^{-\epsilon}\;\Gamma(1+\epsilon)\left[\frac{2}{\epsilon^2}\;+\;\frac{7}{2\epsilon}\right]\not\epsilon\not p'\not k\;+\ldots \quad . \tag{3.31}$$

The appendix contains a tabulation of the relevant contractions with $T^{(1)\alpha\beta\gamma\delta}$. Using the results given there

$$J^{(1)}\;+\;J^{(2)} \;=\; -\frac{1}{(16\pi^2)^{n/2}}\,(-p^2)^{-\epsilon}\;\Gamma(1+\epsilon)\;\left[\frac{-4}{9\epsilon^2}\;-\;\frac{61}{27\epsilon}\right]\not\epsilon p\cdot k\;+\ldots \quad . \tag{3.32}$$

Next consider the graphs in Fig. 10. In Feynman gauge they give

$$\frac{4e}{3}\;g^2\;Q_c\;\left[J^{(3)}(p',k)\;+\;J^{(4)}(p,k)\right]\frac{(1-\gamma_5)}{2} \quad . \tag{3.33}$$

In this case

$$J^{(3)}(p',k) = \int\frac{d^nq}{(2\pi)^n}\int\frac{d^nr}{(2\pi)^n}\gamma^\mu\frac{1}{\not p'-\not r}\gamma^\lambda\frac{1}{\not q-\not k}\not\epsilon\frac{1}{\not q}\gamma_\mu\frac{1}{\not q+\not r}\gamma_\lambda\frac{1}{r^2}\,, \tag{3.34}$$

$$J^{(4)}(p,k) = \int\frac{d^nq}{(2\pi)^n}\int\frac{d^nr}{(2\pi)^n}\gamma^\lambda\frac{1}{\not q+\not r}\gamma^\mu\frac{1}{\not q}\not\epsilon\frac{1}{\not q+\not k}\gamma_\lambda\frac{1}{\not p-\not r}\gamma_\mu\frac{1}{r^2}\,. \tag{3.35}$$

$J^{(3)}$ and $J^{(4)}$ are related in precisely the same way as $J^{(1)}$ and $J^{(2)}$ so the discussion between eqs. (3.19) and (3.26) applies with $J^{(1)}$ and $J^{(2)}$ replaced by $J^{(3)}$ and $J^{(4)}$, respectively. Moreover, writing

$$J^{(3)} = J^{(3)}_{\alpha\beta\gamma\delta} \, T^{(3)\alpha\beta\gamma\delta} \quad , \tag{3.36}$$

with

$$T^{(3)\alpha\beta\gamma\delta} = \gamma^\mu \gamma^\alpha \gamma^\lambda \gamma^\beta \not{\epsilon} \, \gamma^\gamma \gamma_\mu \gamma^\delta \gamma_\lambda \quad , \tag{3.37}$$

and expanding to linear order in k yields

$$J^{(3)}_{\alpha\beta\gamma\delta} = 2k^\rho \, K^{(1a)}_{\alpha\delta\gamma\beta\rho} - k_\beta \, K^{(1b)}_{\alpha\delta\gamma} - K^{(1c)}_{\alpha\delta\gamma\beta} \quad . \tag{3.38}$$

Note that no new integrals are encountered. The contractions of $T^{(3)}$ with the relevant tensors are listed in the appendix. Using these and the values of the integrals gives the divergent contribution

$$J^{(3)} + J^{(4)} = -\frac{1}{(16\pi^2)^{n/2}} (-p^2)^{-\epsilon} \, \Gamma(1+\epsilon) \left[\frac{4}{9\epsilon^2} + \frac{169}{27\epsilon} \right] \not{\epsilon} p \cdot k + \ldots \quad . \tag{3.39}$$

The last pair of truly two–loop graphs that make a contribution to the mixing of O_2 with Q_3 are shown in Fig. 11. In Feynman gauge they give

$$\frac{4}{3} e g^2 \, Q_b \left[J^{(5)}(p', k) + J^{(6)}(p, k) \right] \frac{(1-\gamma_5)}{2} \quad , \tag{3.40}$$

where $Q_b = -1/3$ is the charge of the bottom quark and

$$J^{(5)}(p', k) = \int \frac{d^n q}{(2\pi)^n} \int \frac{d^n r}{(2\pi)^n} \gamma^\mu \frac{1}{\not{r} + \not{p}'} \not{\epsilon} \frac{1}{\not{p}' + \not{r} + \not{k}} \gamma^\lambda \frac{1}{\not{q} + \not{r}} \gamma_\mu \frac{1}{\not{q}} \gamma_\lambda \frac{1}{r^2} \, , \tag{3.41}$$

$$J^{(6)}(p,k) = \int \frac{d^n q}{(2\pi)^n} \int \frac{d^n r}{(2\pi)^n} \gamma^\lambda \frac{1}{\not q} \gamma^\mu \frac{1}{\not q + \not r} \gamma_\lambda \frac{1}{\not r + \not p - \not k} \not\epsilon \frac{1}{\not r + \not p} \gamma_\mu \frac{1}{r^2} \ . \quad (3.42)$$

The relationship between $J^{(5)}$ and $J^{(6)}$ is the same as between $J^{(1)}$ and $J^{(2)}$ given in eq. (3.29). Again the discussion between eqs. (3.19) and (3.26) applies, but this time with $J^{(1)}$ and $J^{(2)}$ replaced by $J^{(5)}$ and $J^{(6)}$, respectively. Writing

$$J^{(5)} = J^{(5)}_{\alpha\beta\gamma\delta}\ T^{(5)\alpha\beta\gamma\delta} \quad , \quad (3.43)$$

with

$$T^{(5)\alpha\beta\gamma\delta} \ = \ \gamma^\mu \gamma^\alpha \not\epsilon \gamma^\beta \gamma^\lambda \gamma^\gamma \gamma_\mu \gamma^\delta \gamma_\lambda \quad , \quad (3.44)$$

gives, upon expanding to linear order in k, that

$$J^{(5)}_{\alpha\beta\gamma\delta} \ = \ -2k^\rho\ K^{(5a)}_{\alpha\beta\gamma\delta\rho} \ + \ k_\beta\ K^{(5b)}_{\alpha\gamma\delta} \ + \ K^{(5c)}_{\alpha\beta\gamma\delta} \quad , \quad (3.45)$$

where

$$K^{(5a)}_{\alpha\beta\gamma\delta\rho} = \int \frac{d^n r}{(2\pi)^n} \int \frac{d^n q}{(2\pi)^n} \frac{(r+p')_\alpha (r+p')_\beta (q+r)_\gamma q_\delta (r+p')_\rho}{r^2[(r+p')^2]^3 (q+r)^2 q^2} \quad , (3.46a)$$

$$K^{(5b)}_{\alpha\gamma\delta} = \int \frac{d^n r}{(2\pi)^n} \int \frac{d^n q}{(2\pi)^n} \frac{(r+p')_\alpha (q+r)_\gamma q_\delta}{r^2[(r+p')^2]^2 (q+r)^2 q^2} \quad , \quad (3.46b)$$

$$K^{(5c)}_{\alpha\beta\gamma\delta} = \int \frac{d^n r}{(2\pi)^n} \int \frac{d^n q}{(2\pi)^n} \frac{(r+p')_\alpha (r+p')_\beta (q+r)_\gamma q_\delta}{r^2[(r+p')^2]^2 (q+r)^2 q^2} \quad . \quad (3.46c)$$

The contribution of Fig. 11 to the mixing of O_2 with Q_3 is extracted from the $\not\epsilon \not p' \not k$ and the $\not\epsilon p'^2$ terms in $J^{(5)}$ as in eqs. (3.20) and (3.25). Only for $J^{(5)} + J^{(6)}$ is the $\epsilon\gamma_0$ piece in eq. (3.25) important. The $1/\epsilon^2$ pole in $J^{(1)} + J^{(2)}$ cancels against that for $J^{(3)} + J^{(4)}$

separately for β_0 and γ_0. On the other hand, in $J^{(5)}$ and $J^{(6)}$ the $1/\epsilon^2$ pole vanishes due to a cancellation between the β_0 and γ_0 contributions. The cancellation of the $1/\epsilon^2$ poles must occur because although we are computing a two–loop contribution to the anomalous dimension matrix, it is a leading logarithmic term since the one–loop mixing vanishes. Expressions for the integrals $K^{(5a,b,c)}$ and the relevant contractions with $T^{(5)}$ can be found in the appendix. They give, for the divergent piece,

$$J^{(5)} \; + \; J^{(6)} \;=\; -\frac{1}{(16\pi^2)^{n/2}}\,(-p^2)^{-\epsilon}\,\Gamma(1+\epsilon)\left[\frac{-4}{9\epsilon}\right] \not{\epsilon} p\cdot k \;+\ldots \quad . \tag{3.47}$$

To complete our calculation of the mixing of O_2 into Q_3 the contributions from the graphs in Figs. 12 are required. In these one–loop diagrams the vertex denoted by the shaded square arises from the one–loop counterterm to O_2 that is proportional to Q_5. The counterterm is computed from Fig. 16 and the resulting vertex is

$$-\frac{1}{16\pi^2}\,\frac{4}{3}\,g\,T^a\,\frac{1}{\epsilon}\,(k^2\gamma^\gamma - k^\gamma \not{k}) \quad . \tag{3.48}$$

Fig. 12 gives the contribution (in Feynman gauge)

$$\frac{i}{16\pi^2\epsilon}\,Q_b\,\frac{16}{9}\,eg^2\left[J^{(7)} + J^{(8)}\right]\frac{(1-\gamma_5)}{2} \quad , \tag{3.49}$$

where

$$J^{(7)} \;=\; \int \frac{d^n q}{(2\pi)^n}\,\gamma^\gamma\,\frac{1}{(\not{q}+\not{p}-\not{k})}\,\not{\epsilon}\,\frac{1}{(\not{q}+\not{p})}\,\gamma^\delta\left(\frac{q^2\eta_{\gamma\delta} - q_\gamma q_\delta}{q^2}\right) \quad , \tag{3.50}$$

and

$$J^{(8)} \;=\; J^{(7)} \quad . \tag{3.51}$$

Expanding to linear order in k we write

$$J^{(7)} = T^{(7)\gamma\alpha\beta\delta} \, J^{(7)}_{\alpha\beta\gamma\delta} \quad , \tag{3.52}$$

where

$$T^{(7)\gamma\alpha\beta\delta} = \gamma^\gamma \, \gamma^\alpha \, \not{q} \, \gamma^\beta \gamma^\delta \quad , \tag{3.53}$$

and

$$J^{(7)}_{\alpha\beta\gamma\delta} = 2k^\rho \, K^{(7a)}_{\alpha\beta\gamma\delta\rho} - k_\alpha \, K^{(7b)}_{\beta\gamma\delta} \quad . \tag{3.54}$$

The integrals $K^{(7a,b)}$ are

$$K^{(7a)}_{\alpha\beta\gamma\delta\rho} = \int \frac{d^n q}{(2\pi)^n} \, \frac{(p+q)_\alpha (p+q)_\beta (q^2 \eta_{\gamma\delta} - q_\gamma q_\delta)(p+q)_\rho}{[(p+q)^2]^3 \, q^2} \, , \tag{3.55a}$$

$$K^{(7b)}_{\beta\gamma\delta} = \int \frac{d^n q}{(2\pi)^n} \, \frac{(p+q)_\beta (q^2 \eta_{\gamma\delta} - q_\gamma q_\delta)}{[(p+q)^2]^2 \, q^2} \quad . \tag{3.55b}$$

Since

$$K^{(7b)}_{\beta\gamma\delta} = \eta^{\alpha\rho} \, K^{(7a)}_{\alpha\beta\gamma\delta\rho} \quad , \tag{3.56}$$

there is only one integral to compute. The appendix gives this integral and the relevant contractions with $T^{(7)}$. Using these results we find the convergent result

$$J^{(7)} + J^{(8)} = \frac{-i}{16\pi^2} \, \not{p} p \cdot k \quad . \tag{3.57}$$

Next we consider the mixing of O_2 with the $(\bar{5}_L, 5_R)$ operator Q_8. In Feynman gauge Figs. 13 give the contribution

$$\frac{4}{3}\ m_b e g^2\ Q_c[J^{(9)} + J^{(10)}]\frac{(1+\gamma_5)}{2} \quad , \tag{3.58}$$

where

$$J^{(9)} \ = \ \int \frac{d^n q}{(2\pi)^n} \int \frac{d^n r}{(2\pi)^n}\ \gamma^\mu \frac{1}{\not q - \not k}\ \not \epsilon\ \frac{1}{\not q}\ \gamma^\lambda\ \frac{1}{\not q + \not r}\ \gamma_\mu \gamma_\lambda \frac{1}{(r+p)^2}\ \frac{1}{r^2}\ , \tag{3.59}$$

and

$$J^{(10)} \ = \ \int \frac{d^n q}{(2\pi)^n} \int \frac{d^n r}{(2\pi)^n}\ \gamma^\mu \frac{1}{\not q + \not r}\ \gamma^\lambda\ \frac{1}{\not q}\ \not \epsilon\ \frac{1}{\not q + \not k}\ \gamma_\mu \gamma_\lambda\ \frac{1}{(r-p)^2}\ \frac{1}{r^2} \quad . \tag{3.60}$$

The only Lorentz structure that is relevant is $\not\epsilon \not k$ so we expand in the external momentum k, keeping only the linear piece. This gives for $J^{(9)}$

$$J^{(9)} \ = \ T^{(9)\alpha\beta\gamma}\ J^{(9)}_{\alpha\beta\gamma} \quad , \tag{3.61}$$

where

$$T^{(9)\alpha\beta\gamma} \ = \ \gamma^\mu \gamma^\alpha \not\epsilon \gamma^\beta \gamma^\lambda \gamma^\gamma \gamma_\mu \gamma_\lambda \quad , \tag{3.62}$$

and

$$J^{(9)}_{\alpha\beta\gamma} \ = \ 2k^\rho\ K^{(9a)}_{\alpha\beta\gamma\rho}\ -\ k_\alpha\ K^{(9b)}_{\beta\gamma} \quad . \tag{3.63}$$

In eqs. (3.63) the integrals $K^{(9a)}$ and $K^{(9b)}$ are

$$K^{(9a)}_{\alpha\beta\gamma\rho} \ = \ \int \frac{d^n q}{(2\pi)^n} \int \frac{d^n r}{(2\pi)^n}\ \frac{q_\alpha q_\beta (q+r)_\gamma q_\rho}{(q^2)^3 (q+r)^2 (r+p)^2 r^2} \quad , \tag{3.64}$$

$$
\begin{aligned}
K^{(9b)}_{\beta\gamma} &= \int \frac{d^n q}{(2\pi)^n} \int \frac{d^n r}{(2\pi)^n} \frac{q_\beta (q+r)_\gamma}{(q^2)^2 (q+r)^2 (r+p)^2 r^2} \\
&= \eta^{\alpha\rho}\, K^{(9a)}_{\alpha\beta\gamma\rho} \quad .
\end{aligned} \tag{3.65}
$$

For $J^{(10)}$, expanding in k and keeping only the linear piece gives

$$
J^{(10)} = T^{(10)\alpha\beta\gamma}\, J^{(10)}_{\alpha\beta\gamma} \quad , \tag{3.66}
$$

where

$$
T^{(10)\alpha\beta\gamma} = \gamma^\lambda \gamma^\alpha \gamma^\mu \gamma^\beta \not{\epsilon} \gamma^\gamma \gamma_\lambda \gamma_\mu \quad , \tag{3.67}
$$

and

$$
J^{(10)}_{\alpha\beta\gamma} = -2k^\rho\, K^{(9a)}_{\gamma\beta\alpha\rho} + k_\gamma\, K^{(9b)}_{\beta\alpha} \quad . \tag{3.68}
$$

Note that no new integrals enter the computation of $J^{(10)}$. The results of the appendix give, for the divergent contribution,

$$
J^{(9)} = -\frac{1}{(16\pi^2)^{n/2}} (-p^2)^{-\epsilon}\, \Gamma(1+\epsilon) \left[\frac{2}{\epsilon}\right] \not{\epsilon}\not{k} + \ldots \quad , \tag{3.69}
$$

$$
J^{(10)} = 0\, \not{\epsilon}\not{k} + \ldots \quad . \tag{3.70}
$$

The last truly two–loop Feynman diagrams to be considered are those of Fig. 14. Here we encounter a problem if m_b is treated as a perturbation. With three b–quark propagators these graphs are "infrared" divergent as the gluon momentum approaches $-p$. Therefore instead of expanding about $m_b = 0$ we keep the bottom quark mass in the propagators but now expand to zeroth order in p and linear order in k. Then

Fig. 14 gives the contribution

$$m_b e g^2 \, \frac{4}{3} \, Q_b \, J^{(11)} \, \frac{(1+\gamma_5)}{2} \quad , \tag{3.71}$$

where

$$J^{(11)} \;=\; -4 \, \epsilon^\gamma \, k^\rho \, T^{(11a)\alpha\beta} \, K^{(11a)}_{\alpha\beta\gamma\rho} \;+\; T^{(11b)\alpha\beta\gamma\rho} \, K^{(11b)}_{\alpha\beta} \quad , \tag{3.72}$$

with

$$T^{(11a)\alpha\beta} = \gamma^\lambda \gamma^\alpha \gamma^\mu \gamma^\beta \gamma_\lambda \gamma_\mu \quad , \tag{3.73a}$$

$$T^{(11b)\alpha\beta} = \gamma^\lambda \gamma^\alpha \gamma^\mu \gamma^\beta \gamma_\lambda \not{k} \not{\epsilon} \gamma_\mu \quad , \tag{3.73b}$$

and

$$K^{(11a)}_{\alpha\beta\gamma\rho} = \int \frac{d^n q}{(2\pi)^n} \, \frac{d^n r}{(2\pi)^n} \, \frac{q_\alpha (q+r)_\beta r_\gamma r_\rho}{(q^2)(q+r)^2 r^2 (r^2 - m_b^2)^3} \quad , \tag{3.74a}$$

$$K^{(11b)}_{\alpha\beta} = \int \frac{d^n q}{(2\pi)^n} \, \frac{d^n r}{(2\pi)^n} \, \frac{q_\alpha (q+r)_\beta}{(q^2)(q+r)^2 r^2 (r^2 - m_b^2)^2} \quad . \tag{3.74b}$$

Using the results listed in the appendix, one finds

$$J^{(11)} \;=\; -\frac{1}{(16\pi^2)^{n/2}} \, (m_b^2)^{-\epsilon} \, \Gamma(1+\epsilon) \left[\frac{-1}{\epsilon} \right] \not{\epsilon} \not{k} \; + \ldots \quad . \tag{3.75}$$

The last contribution to the mixing of O_2 into Q_8 are the one-loop diagrams in Fig. 15, which contain an insertion of the one-loop counterterm (3.48). As was the case for the diagrams in Fig. 14, this is best computed by setting $p = 0$ and keeping the b–quark mass in the propagator to regulate possible infrared divergences. Then one picks out the term that flips chirality and expands in k keeping only the linear term. This procedure yields for the graphs in Fig. 15

$$\frac{i}{16\pi^2}\,\frac{16}{9}\,eg^2\,Q_b\,\frac{1}{\epsilon}\,m_b\,J^{(12)}\,\frac{(1+\gamma_5)}{2} \quad , \tag{3.76}$$

where

$$J^{(12)} \;=\; -4(n-1)\,\epsilon^{\alpha}\,k^{\beta}\,K^{(12a)}_{\alpha\beta} \;+\; \gamma^{\alpha}\,\not{k}\not{\epsilon}\,\gamma^{\beta}\,K^{(12b)}_{\alpha\beta} \quad , \tag{3.77}$$

with

$$\begin{aligned} K^{(12a)}_{\alpha\beta} &= \int \frac{d^n q}{(2\pi)^n}\,\frac{q_\alpha q_\beta}{(q^2-m_b^2)^3} \\ &= \frac{i}{(16\pi^2)^{n/4}}\,(m_b^2)^{-\epsilon/2}\,\frac{1}{2}\,\Gamma(1+\epsilon/2)\,\frac{1}{\epsilon}\,\eta_{\alpha\beta} \quad , \end{aligned} \tag{3.78a}$$

and

$$\begin{aligned} K^{(12b)}_{\alpha\beta} &= \int \frac{d^n q}{(2\pi)^n}\,\frac{q^2\eta_{\alpha\beta}-q_\alpha q_\beta}{q^2(q^2-m_b^2)^2} \\ &= \frac{i}{(16\pi^2)^{n/4}}\,(m_b^2)^{-\epsilon/2}\,\Gamma(1+\epsilon/2)\,\frac{2}{\epsilon}\left(1-\frac{1}{n}\right)\eta_{\alpha\beta} \quad . \end{aligned} \tag{3.78b}$$

It follows that the divergent part of (3.76) with the Lorentz structure $\not{\epsilon}\not{k}$ is determined from

$$J^{(12)} \;=\; \frac{i}{16\pi^2}\,\frac{3}{4}\,\not{\epsilon}\not{k}\;+\ldots \quad . \tag{3.79}$$

This completes the calculations that give the Q_3 and Q_8 counterterms to O_2.

The renormalized operators $O_j(\mu)$, $j = 1,\ldots,8$ are related to the bare μ–independent operators $O_j^{(0)}, j = 1,\ldots 8$, via the relation

$$O_j(\mu) \;=\; \sum_{i=1}^{8}\,\mu^{\epsilon D_j}\,Z_{ji}\,\mu^{-\epsilon D_i^{(0)}}\,O_i^{(0)} \quad , \tag{3.80}$$

where Z_{ji} is dimensionless and has the perturbative expansion

$$Z_{ij} \;=\; \delta_{ij} \;+\; \frac{g^2}{8\pi^2\epsilon}\, Z^{(1)}_{ij} \;+\ldots \quad . \tag{3.81}$$

As stated in Chapter 2, the factors of $\mu^{\epsilon D_j}$ and $\mu^{-\epsilon D^{(0)}_j}$ in eq. (3.80) arise because in dimensional regularization the operators O_1–O_8 and $O^{(0)}_1$–$O^{(0)}_8$ don't all have the same dimension.

$$\epsilon D_j = \text{ dimension } [O_j] \;-\; (2n-2) \quad , \tag{3.82a}$$

and

$$\epsilon D^{(0)}_j = \text{ dimension } [O^{(0)}_j] \;-\; (2n-2) \quad . \tag{3.82b}$$

Using the eqs. of motion to relate Q_3 and Q_8 to the electromagnetic magnetic moment operator O_7 we deduce that

$$Z^{(1)}_{27} \;=\; \Big(-2Q_c \;+\; \frac{8}{27}\, Q_b\Big) \quad . \tag{3.83}$$

The anomalous dimension matrix follows from eq. (3.80) and as was noted in Chapter 2 it has the perturbative expansion

$$\gamma_{ij}(g) \;=\; \frac{-g^2}{8\pi^2}\, Z^{(1)}_{ij}\, (1 + D^{(0)}_j \;-\; D^{(0)}_i) \;+\ldots \quad , \tag{3.84}$$

where

$$D^{(0)}_i \;=\; \begin{cases} 0 & i = 1,\ldots,6 \\ 1 & i = 7,8 \quad . \end{cases} \tag{3.85}$$

Combining eqs. (4.1), (3.83), (3.84), and (3.85) gives

$$X_2 \;=\; \Big(4Q_c \;-\; \frac{16}{27}\, Q_b\Big) \;=\; \frac{232}{81} \quad . \tag{3.86}$$

There have been other attempts to compute X_2. In ref. [3.2] the part of X_2 proportional to Q_c was calculated by working on–shell in four–dimensions and extracting the logarithmic ultraviolet divergence. Our result agrees with theirs. Ref. [3.4] calculated X_2 using dimensional reduction. They find a value for X_2 that disagrees with ours. We believe that the origin of this discrepancy lies in the inability to straightforwardly apply dimensional reduction as a regulator for non–supersymmetric gauge theories [3.6]. In a more recent publication, Ref. [3.7], the authors find that indeed dimensional reduction is invalid for this calculation.

References for Chapter 3

3.1. F.J. Gilman and M.B. Wise, Phys. Rev. **D20** (1979) 2392.

3.2. M.A. Shifman, A.I. Vainshtein and V.I. Zakharov, Phys. Rev. **D18** (1978) 2583.

3.3. B. Grinstein, R. Springer and M.B. Wise, Phys. Lett. **B202** (1988) 138.

3.4. R. Grigjanis, P.J. Odonnell, M. Sutherland and H. Navelet, Phys. Lett. **B213** (1988) 355.

3.5. D.J. Gross and F. Wilczek, Phys. Rev. Lett. **30** (1973) 1343; H.D. Politzer, Phys. Rev. Lett. **30** (1973) 1346.

3.6. R. Van Damme and G. 'tHooft, Phys. Lett. **B150** (1985) 133.

3.7. R. Grigjanis, P.J. O'Donnell, M. Sutherland and H. Navelet, Phys. Lett. **B237** (1990) 252.

Chapter 4. Truncation of the Anomalous Dimension Matirx

To find the $b \to s\gamma$ decay rate, we used not the full anomalous dimension matrix, but an abbreviated version. This is justified in what follows.

The anomalous dimension matrix for the mixing of the operators O_1–O_8 has the form (eq. (3.4))

$$\gamma = \frac{g^2}{8\pi^2}\begin{pmatrix} -1 & 3 & 0 & 0 & 0 & 0 & 0 & Y_1 \\ 3 & -1 & -1/9 & 1/3 & -1/9 & 1/3 & X_2 & Y_2 \\ 0 & 0 & -11/9 & 11/3 & -2/9 & 2/3 & X_3 & Y_3 \\ 0 & 0 & 22/9 & 2/3 & -5/9 & 5/3 & X_4 & Y_4 \\ 0 & 0 & 0 & 0 & 1 & -3 & X_5 & Y_5 \\ 0 & 0 & -5/9 & 5/3 & -5/9 & -19/3 & X_6 & Y_6 \\ 0 & 0 & 0 & 0 & 0 & 0 & 16/3 & 0 \\ 0 & 0 & 0 & 0 & 0 & 0 & -16/9 & 14/3 \end{pmatrix} . \tag{4.1}$$

If the mixing of O_2 with the other four quark operators and with the gluon magnetic moment operator O_8 is neglected then eq. (2.24) yields

$$\begin{aligned} C_7(m_b) = \left[\frac{\alpha_s(M_W)}{\alpha_s(m_b)}\right]^{16/23} & \left\{ C_7(M_W) - \frac{8}{3}\, C_8(M_W)\left[1 - \left(\frac{\alpha_s(m_b)}{\alpha_s(M_W)}\right)^{2/23}\right]\right. \\ & \left. + \frac{3X_2}{19}\left[1 - \left(\frac{\alpha_s(m_b)}{\alpha_s(M_W)}\right)^{19/23}\right]\right\} . \end{aligned} \tag{4.2}$$

In the last section it was shown that

$$X_2 = \frac{232}{81} . \tag{4.3}$$

It is now known that the t–quark is quite heavy. In the minimal standard model, when $m_t = M_W$, the matching conditions $C_7(M_W)$ and $C_8(M_W)$ have the values

$C_7(M_W) \simeq -0.1$ and $C_8(M_W) \simeq -0.06$ respectively. To evaluate the various terms in the eq. (4.2) we also need the value of the strong coupling (at m_b and M_W). In the leading logarithmic approximation $\alpha_s(M)$ has the form

$$\alpha_s(M) = \frac{12\pi}{(33 - 2N_f)\ell n(M^2/\Lambda^2_{\rm QCD})} \quad , \tag{4.4}$$

where $N_f = 5$ is the number of quark flavors appropriate to the low energy effective five quark theory. Experimentally, it has been determined that $\Lambda_{\rm QCD}$ lies between 100 MeV and 300 MeV [G. Yost et al. (Particle Data Group), Phys. Lett. **B204** (1988) 1]. For $\Lambda_{\rm QCD} = 100$ MeV, $\alpha_s(M_W) = 0.12$ and $\alpha_s(m_b) = 0.21$. Numerically the expression for $C_7(m_b)$, in the minimal standard model (with $m_t = M_W$, $\Lambda_{\rm QCD} =$ 100 MeV) becomes

$$\begin{aligned} C_7(m_b) &\simeq 0.68\{-0.1 - 0.008 - 0.27\} \\ &\simeq -0.26 \quad . \end{aligned} \tag{4.5}$$

The three terms in the brace brackets of eq. (4.5) are in correspondence with those of eq. (4.2). The term proportional to $C_8(M_W)$ makes only a 2% contribution to $C_7(m_b)$. Also, eq. (4.5) shows that, in the minimal standard model with $m_t = M_W$ (and $\Lambda_{\rm QCD} = 100$ MeV), strong interaction effects increase the rate for weak radiative $\bar{B}$–meson decay by about a factor of seven. For $\Lambda_{\rm QCD} = 300$ MeV, $\alpha_s(M_W) = 0.15$ and $\alpha_s(m_b) = 0.29$. This gives, for $m_t = M_W$, $C_7(m_b) \simeq -0.27$ and so experimental uncertainties in the value of $\Lambda_{\rm QCD}$ only have a small affect on the rate for weak radiative $\bar{B}$–meson decay.

The truncation of the anomalous dimension matrix used to derive eq. (4.2) is an additional approximation beyond the leading logarithmic approximation. It correctly gives the $[\alpha_s(m_b)/\pi]\ell n(m_t^2/m_b^2)$ term in the perturbative expansion of $C_7(m_b)$ but misses some contributions to the $\{[\alpha_s(m_b)/\pi]\ell n(m_t^2/m_b^2)\}^p$ terms for $p \geq 2$. Despite this we expect that eq. (4.2) will prove to be quite an accurate approximation to $C_7(m_b)$. In this chapter we explore the accuracy of eq. (4.2) by studying, in three examples, the effect of some of the terms in the anomalous dimension matrix that were neglected in eq. (4.2).

(*i*) In deriving eq. (4.2) the mixing of O_2 with O_1 (and the other four–quark operators) was neglected. If we include the mixing between O_2 and O_1 (but neglect the mixing of O_1 with the gluon magnetic moment operator) then the term proportional to X_2 in the brace brackets of eq. (4.2) becomes

$$\frac{3X_2}{20}\left[1-\left(\frac{\alpha_s(m_b)}{\alpha_s(M_W)}\right)^{10/23}\right]+\frac{3X_2}{56}\left[1-\left(\frac{\alpha_s(m_b)}{\alpha_s(M_W)}\right)^{28/23}\right] . \qquad (4.6)$$

This is the form used in our original work. It looks quite different from the term proportional to X_2 in eq. (4.2). However, numerically, the two expressions are quite close (i.e., within 1% of each other). Thus the mixing between O_2 and O_1 has negligible impact on the value of $C_7(m_b)$.

(*ii*) Suppose the mixing of O_2 with the operator O_6 was not neglected. Then (neglecting the mixing of O_6 with the gluon magnetic moment operator and with the other four–quark operators) there would be the following additional contribution to the brace brackets of eq. (4.2)

$$\frac{-3X_6}{304}\left[\left(\frac{\alpha_s(m_b)}{\alpha_s(M_W)}\right)^{19/23}-1\right]+\frac{3X_6}{560}\left[\left(\frac{\alpha_s(m_b)}{\alpha_s(M_W)}\right)^{35/23}-1\right] . \qquad (4.7)$$

In order for this term to be a 15% correction to $C_7(m_b)$ the magnitude of X_6 must be about 40 (in the minimal standard model with $m_t = M_W$ and $\Lambda_{\rm QCD} = 100$ MeV). This is an unreasonably large value and so we feel confident that the mixing of O_2 with O_6 has negligible impact on the value of $C_7(m_b)$. The mixing of O_2 with the other four quark operators O_3, O_4, and O_5 is even less significant.

(*iii*) As our final example we suppose that the mixing of O_2 with the gluon magnetic moment operator O_8 had not been neglected. If this were the case then the brace brackets of eq. (4.2) would contain the additional term

$$\frac{8Y_2}{17}\left[\left(\frac{\alpha_s(m_b)}{\alpha_s(M_W)}\right)^{2/23}-1\right] - \frac{16Y_2}{323}\left[\left(\frac{\alpha_s(m_b)}{\alpha_s(M_W)}\right)^{19/23}-1\right] \quad . \tag{4.8}$$

In the minimal standard model (with $m_t = M_W$ and $\Lambda_{\rm QCD} = 100$ MeV) this term is less than a 15% correction to the value of $C_7(m_b)$, provided $|Y_2| \leq 10$ (a rather large value).

The three examples discussed above give us confidence that in the minimal standard model, the error in $C_7(m_b)$, incurred by our truncation of the anomalous dimension matrix, is less than 15%.

Chapter 5. Conclusions and Prospects

Modelling weak radiative $\bar{B}$–meson decay by b–quark decay gives, in the leading logarithmic approximation, the inclusive rate

$$\Gamma(\bar{B} \to X_s\gamma) \;=\; (s_2^2 + s_3^2 + 2s_2s_3c_\delta)\,\frac{G_F^2 m_b^5 \alpha_{em}}{32\pi^4}\,|C_7(m_b)|^2 \quad . \tag{5.1}$$

In the previous sections we have computed $C_7(m_b)$ in the minimal standard model. The sensitive dependence of the rate for weak radiative $\bar{B}$–meson decay on the b–quark mass, and its dependence on the weak mixing angles, can be removed by normalizing it to the measured semileptonic $\bar{B}$–meson decay rate; $Br(\bar{B} \to Xe\bar{\nu}_e) = (12.3 \pm 0.8)\%$. Modelling semileptonic $\bar{B}$–meson decay by b–quark decay (and neglecting the small contribution from $b \to u$ transitions) gives

$$\Gamma(\bar{B} \to Xe\bar{\nu}_e) \;=\; (s_2^2 + s_3^2 + 2s_2s_3c_\delta)\,\frac{G_F^2 m_b^5}{192\pi^3}\, f(m_c/m_b) \quad , \tag{5.2}$$

where

$$f(x) \;=\; 1 \;-\; 8x^2 \;+\; 8x^6 \;-\; x^8 \;-\; 24x^4\,\ell n x \quad . \tag{5.3}$$

The function $f(x)$ takes into account the effect on the semileptonic decay rate of the charm quark mass. For $m_b = 4.5$ GeV and $m_c = 1.5$ GeV, $f(m_c/m_b) = 0.44$.

Combining equations (5.1) and (5.2) gives

$$\frac{\Gamma(\bar{B} \to X_s\gamma)}{\Gamma(\bar{B} \to Xe\bar{\nu}_e)} \;=\; \left[\frac{6\alpha_{em}}{\pi f(m_c/m_b)}\right] |C_7(m_b)|^2 \quad . \tag{5.4}$$

Fig. 17 shows a plot of this ratio, for the minimal standard model, as a function of the top quark mass, for $\Lambda = 100$ MeV. The rate is insensitive to uncertainties in the value of Λ_{QCD}. The dashed line is the decay rate when strong interaction effects are not included. Note that the effect of the strong interaction corrections on the decay rate is very dramatic at smaller top quark masses. This is because, when strong interactions are neglected, there is a GIM cancellation [5.1] that causes $C_7(m_b)$ to go as (m_t^2/M_W^2) for small m_t. The strong interaction corrections, on the other hand, have only a logarithmic GIM cancellation. Even for large m_t the leading logarithmic strong interaction effects are important. For example, when $m_t = 120$ GeV they increase the inclusive rate for weak radiative $\bar{B}$–meson decay by about a factor of four. We expect that the next–to–leading logarithmic corrections, which are suppressed by a factor of $\alpha_s(m_b)/\pi$, lead to about a 20% uncertainty in the prediction for the decay rate presented in Fig. 17.

The above decay rate is the one that the Standard Model predicts. This awaits confirmation with experiment. Within the next few years, the B factory at Cornell may be able to measure inclusive decay rates to the 10^{-4} level, and expects to be able to measure several exclusive decay rates to the 10^{-5} level. The calculation that we have done is really useful only for inclusive predictions. This is true because, as discussed earlier, the exclusive rate for the first resonance to be reached (the $K^*(890)$) is quite suppressed. Further, the breakdown of our inclusive prediction into exclusive modes requires the use of form factors that are not well known. Judging from analogous calculations for semileptonic decay, the free quark inclusive decay rate may differ from the full B–meson decay rate by as much as 30 percent.

If the minimal Standard Model is not correct, but involves another Higgs doublet, this scenario can be incorporated into the method described here. With a second Higgs doublet, there will be another physical charged particle (in addition to the W) that can be exchanged in our matching conditions graphs. This extended Standard

Model will result in modifications of our initial conditions $C_7(M_W)$ and $C_8(M_W)$, but the rest of the calculation proceeds as before. The operator list is the same and so is the anomalous dimension matrix. This calculation of the $\overline{B} \to X_s\gamma$ decay rate in the Standard Model with two Higgs doublets was done in Ref.[5.2].

Another attractive model that shows promise of solving the hierarchy puzzle is Supersymmetry[5.3]. Supersymmetry requires that each fermion particle have a boson partner and each boson particle have a fermion partner. What this means for us and our $b \to s\gamma$ decay rate is extra particles that can participate in our matching condition graphs. Again, this modifies $C_7(M_W)$ and $C_8(M_W)$, but the rest of the procedure is the same. This calculation is in progress now (with Martin Savage).

References for Chapter 5

5.1. S.L. Glashow, J. Iliopoulos and L. Maiani, Phys. Rev. **D2** (1970) 1285.

5.2. B. Grinstein and M.B. Wise, Phys. Lett. **B201** (1988) 274.

5.3. *Supersymmetry and Supergravity, a reprint volume of Phys. Rep.*, ed. M. Jacob (North-Holland/ World Scientific, 1986).

Figure Captions

1. Some tree level Feynman diagrams that contribute to weak radiative B–meson decay.

2. Quark line diagram for exclusive decay $\bar{B} \to K^{*}\gamma$. A large momentum must be transferred to the spectator quark.

3. Feynman diagrams that determine the one–loop $b \to s\gamma$ decay amplitude.

4. Plot of function, $A(x)$, which determines $C_7(M_W)$ in the standard model with a minimal Higgs sector.

5. Feynman diagrams used to calculate the matching condition $C_8(M_W)$ in the standard model with a minimal Higgs sector.

6. Plot of function $D(x)$, which determines $C_8(M_W)$ in the standard model with a minimal Higgs sector.

7. One–loop diagram, which does not contribute to the mixing of operator O_2 with Q_3.

8. Two–loop diagrams, which do not contribute to the mixing of the operator O_2 with Q_3 or Q_8.

9. Some two–loop diagrams contributing to the mixing of O_2 with Q_3.

10. Some two–loop diagrams contributing to the mixing of O_2 with Q_3.

11. Some two–loop diagrams contributing to the mixing of O_2 with Q_3.

12. Insertion of one–loop counterterm that contributes to mixing of O_2 with Q_3.

13. Some two–loop diagrams contributing to the mixing of O_2 with Q_8.

14. Some two–loop diagrams contributing to the mixing of O_2 with Q_8.

15. Insertion of one–loop counterterm that contributes to the mixing of O_2 with Q_8.

16. Feynman diagram that gives one–loop counterterm inserted in Figures 14 and 17.

17. Solid line is a plot of the rate for $\bar{B} \rightarrow X_s\gamma$ (normalized to the semileptonic decay rate) versus m_t in the standard model with minimal Higgs sector. The dashed line is a plot of the same quantity when strong interactions are neglected.

Appendix A

Here we list the relevant parts of the integrals that appear in Chapter 3. Also, the results of the gamma matrix algebra that were encountered there are tabulated. For simplicity we introduce the symbols $+(\alpha \to \beta \to \alpha)$, $+(\alpha \to \beta \to \gamma \to \alpha)$ and $+(\alpha \to \beta \to \gamma \to \delta \to \alpha)$ which mean "add cyclic permutations to the tensor" with the corresponding indices. Thus, for example,

$$\begin{aligned}\eta_{\alpha\beta\gamma\delta} &= \eta_{\alpha\beta}\,\eta_{\gamma\delta} \;+\; (\beta \to \gamma \to \delta \to \beta) \\ &= \eta_{\alpha\beta}\,\eta_{\gamma\delta} \;+\; \eta_{\alpha\delta}\,\eta_{\beta\gamma} \;+\; \eta_{\alpha\gamma}\,\eta_{\delta\beta} \quad . \end{aligned} \tag{A.1}$$

For the integrals we introduce $\tilde{K}^{(M)}$ defined by

$$K^{(M)} \;=\; -\,\frac{1}{(16\pi^2)^{n/2}}\,(-\hat{p}^2)^{-\epsilon}\;\Gamma(1+\epsilon)\;\tilde{K}^{(M)} \tag{A.2}$$

for $M = 1a - 5c$ and $9a - 9b$ (here $\hat{p}$ is equal to either p or p');

$$K^{(M)} \;=\; -\,\frac{1}{(16\pi^2)^{n/2}}\,(m_b^2)^{-\epsilon}\;\Gamma(1+\epsilon)\;\tilde{K}^{(M)} \tag{A.3}$$

for $M = 11a - 11b$; and

$$K^{(7a)} \;=\; \frac{i}{(16\pi^2)^{n/4}}\,(-p^2)^{-\epsilon/2}\;\Gamma(1+\epsilon/2)\;\tilde{K}^{(7a)} \quad . \tag{A.4}$$

The expressions for the divergent parts of $\tilde{K}^{(M)}$ in eqs. (A.2) and (A.3) and the value (as $\epsilon \to 0$) of $\tilde{K}^{(7a)}$ in eq. (A.4) are as follows:

$$\tilde{K}^{(1a)}_{\alpha\beta\gamma\delta\rho} = \frac{1}{24\epsilon}\left\{\frac{1}{\epsilon}\Big(1+\frac{17}{6}\epsilon\Big)\ p'_\alpha\ \eta_{\beta\gamma\delta\rho}\ -\ \frac{1}{16}\ p'_\alpha\ \eta_{\beta\gamma\delta\rho}\right.$$

$$+\left[\frac{1}{6}\ \eta_{\delta\rho}\ \Big(\eta_{\alpha\beta}\ p'_\gamma\ +\ \eta_{\alpha\gamma}\ p'_\beta\Big)\ -\ \frac{1}{12}\ \eta_{\beta\gamma}\Big(\eta_{\alpha\delta}\ p'_\rho\ +\ \eta_{\alpha\rho}p'_\delta\Big)\right.$$

$$\left.-\ \frac{1}{6}\ p'_\alpha\ \eta_{\beta\gamma}\ \eta_{\delta\rho}\ +\ \Big(\gamma\to\delta\to\rho\to\gamma\Big)\right]\ +\ \left[\frac{1}{48}\ p'_\beta\ \eta_{\alpha\gamma\delta\rho}\right.$$

$$\left.\left.+\Big(\beta\to\gamma\to\delta\to\rho\to\beta\Big)\right]\right\}\quad , \tag{A.5}$$

$$\tilde{K}^{(1b)}_{\alpha\beta\gamma} = \frac{1}{4\epsilon}\left\{\frac{1}{\epsilon}\Big(1+\frac{29}{12}\epsilon\Big)p'_\alpha\eta_{\beta\gamma}\ +\ \frac{1}{6}\ p'_\beta\eta_{\alpha\gamma}\ +\ \frac{1}{6}\ p'_\gamma\ \eta_{\alpha\beta}\right\}\quad , \tag{A.6}$$

$$\tilde{K}^{(1c)}_{\alpha\beta\gamma\delta} = \frac{1}{36}\left\{p'^2\eta_{\alpha\beta}\ \eta_{\gamma\delta}\Big(-\frac{1}{\epsilon^2}-\frac{83}{24\epsilon}\Big)\ +\ p'^2\Big(\eta_{\alpha\gamma}\ \eta_{\beta\delta}\ +\ \eta_{\alpha\delta}\ \eta_{\beta\gamma}\Big)\right.$$

$$\cdot\ \Big(\frac{1}{2\epsilon^2}\ +\ \frac{17}{12\epsilon}\Big)\ +\ p'_\alpha p'_\beta\ \eta_{\gamma\delta}\Big(-\frac{2}{\epsilon^2}-\frac{59}{12\epsilon}\Big)\ +\ \Big(p'_\alpha p'_\gamma\ \eta_{\beta\delta}$$

$$\left.+\,p'_\alpha p'_\delta\ \eta_{\beta\gamma}\Big)\Big(\frac{1}{\epsilon^2}+\frac{11}{6\epsilon}\Big)+\Big[\eta_{\alpha\beta}\ p'_\gamma p'_\delta+(\beta\to\gamma\to\delta\to\beta)\Big]\left(\frac{1}{4\epsilon}\right)\right\}, \tag{A.7}$$

$$\tilde{K}^{(5a)}_{\alpha\beta\gamma\delta\rho} = \frac{1}{72\epsilon}\left\{-\frac{1}{2}\ \eta_{\gamma\delta}\Big[p'_\alpha\ \eta_{\beta\rho}\ +\ (\alpha\to\beta\to\rho\to\alpha)\Big]\right.$$

$$+\,\frac{3}{4\epsilon}\Big(1+\frac{17}{8}\epsilon\Big)\ (p'_\gamma\ \eta_{\delta\alpha\beta\rho}\ +\ p'_\delta\ \eta_{\gamma\alpha\beta\rho})\ -\frac{1}{4\epsilon}\ \Big(1+\frac{47}{24}\epsilon\Big)\Big[p'_\alpha\ \eta_{\beta\gamma\delta\rho}$$

$$+\,(\alpha\to\beta\to\rho\to\alpha)\Big]\ -\frac{3}{2}\ \frac{p'_\gamma p'_\delta}{p'^2}\Big[p'_\alpha\ \eta_{\beta\rho}\ +\ (\alpha\to\beta\to\rho\to\alpha)\Big]$$

$$-\,\frac{1}{2}\ \frac{p'_\alpha p'_\beta p'_\rho}{p'^2}\ \eta_{\gamma\delta}\ +\ \frac{1}{2p'^2}\ \bigg(\Big[p'_\gamma p'_\alpha p'_\beta\ \eta_{\delta\rho}\ +\ (\alpha\to\beta\to\rho\to\alpha)\Big]$$

$$\left.+\,(\gamma\to\delta\to\gamma)\bigg)\ -\ \frac{p'_\alpha p'_\beta p'_\gamma p'_\delta p'_\rho}{p'^4}\right\}\quad , \tag{A.8}$$

$$\tilde{K}^{(5b)}_{\alpha\gamma\delta} = \frac{1}{6\epsilon}\Bigg\{ -\frac{1}{4}p'_\alpha\ \eta_{\gamma\delta}\ +\ \frac{1}{3\epsilon}\Big(1+\frac{25}{12}\epsilon\Big)(p'_\gamma\ \eta_{\alpha\delta}+p'_\delta\ \eta_{\alpha\gamma})$$
$$-\frac{1}{6\epsilon}\Big(1+\frac{25}{12}\epsilon\Big)\ p'_\alpha\ \eta_{\gamma\delta}-\frac{2}{3}\ \frac{p'_\alpha p'_\gamma p'_\delta}{p'^2}\Bigg\}\quad , \tag{A.9}$$

$$\tilde{K}^{(5c)}_{\alpha\beta\gamma\delta} = \frac{1}{72\epsilon}\Bigg\{p'^2\ \eta_{\alpha\beta}\ \eta_{\gamma\delta}-p'_\alpha p'_\beta\ \eta_{\gamma\delta}\ +\ \frac{1}{2\epsilon}\Big(1+\frac{71}{24}\epsilon\Big)p'^2\ \eta_{\alpha\beta\gamma\delta}$$
$$-\frac{1}{\epsilon}\Big(1+\frac{53}{24}\epsilon\Big)p'_\alpha p'_\beta\ \eta_{\gamma\delta}\ -\frac{3}{\epsilon}\Big(1+\frac{17}{8}\epsilon\Big)\ \eta_{\alpha\beta}\ p'_\gamma p'_\delta$$
$$+\frac{1}{\epsilon}\Big(1+\frac{47}{24}\epsilon\Big)\Big[p'_\alpha p'_\gamma\ \eta_{\beta\delta}\ +\ p'_\alpha p'_\delta\ \eta_{\beta\gamma}\ +\ (\alpha\to\beta\to\alpha)\Big]$$
$$-2\ \frac{p'_\alpha p'_\beta p'_\gamma p'_\delta}{p'^2}\Bigg\}, \tag{A.10}$$

$$\tilde{K}^{(7a)}_{\alpha\beta\gamma\delta\rho} = \frac{1}{24}\Bigg\{ -\frac{1}{2}\ \eta_{\gamma\delta}\ \frac{p_\alpha p_\beta p_\rho}{p^2}\ +\ \Big(-\frac{1}{2\epsilon}-\frac{5}{12}\Big)\Big[\eta_{\alpha\beta\gamma\delta}\ p_\rho$$
$$+(\rho\to\alpha\to\beta\to\rho)\Big]\ +\ \Big(\frac{3}{2\epsilon}+\frac{7}{4}\Big)\Big[p_\gamma\ \eta_{\alpha\beta\rho\delta}\ +\ (\gamma\to\delta\to\gamma)\Big]$$
$$+\frac{1}{2}\Bigg[\frac{p_\alpha p_\beta}{p^2}(p_\gamma\ \eta_{\delta\rho}+p_\delta\ \eta_{\gamma\rho})\ +\ (\rho\to\alpha\to\beta\to\rho)\Bigg]$$
$$-\frac{3}{2}\Bigg[\frac{p_\gamma p_\delta p_\rho}{p^2}\ \eta_{\alpha\beta}\ +\ (\rho\to\alpha\to\beta\to\rho)\Bigg]\ -\ \frac{p_\gamma p_\delta p_\alpha p_\beta p_\rho}{p^4}\Bigg\}\quad , \tag{A.11}$$

$$\tilde{K}^{(9a)}_{\alpha\beta\gamma\rho} = \frac{1}{12\epsilon^2}\Big(1+\frac{17}{12}\epsilon\Big)\ \eta_{\alpha\beta\gamma\rho}\quad , \tag{A.12}$$
$$\tilde{K}^{(9b)}_{\beta\gamma} = \frac{1}{2\epsilon^2}\Big(1+\frac{5}{4}\epsilon\Big)\ \eta_{\beta\gamma}\quad , \tag{A.13}$$
$$\tilde{K}^{(11a)}_{\alpha\beta\gamma\rho} = \frac{-1}{24\epsilon^2}\Bigg\{\Big(1+\frac{7}{12}\epsilon\Big)\ \eta_{\alpha\beta}\ \eta_{\gamma\rho}\ +\ \frac{1}{3}\Big(1+\frac{1}{4}\epsilon\Big)\ \eta_{\alpha\beta\gamma\rho}\Bigg\}\quad , \tag{A.14}$$
$$\tilde{K}^{(11b)}_{\alpha\beta} = -\frac{1}{4\epsilon^2}\Big(1+\frac{3}{4}\epsilon\Big)\ \eta_{\alpha\beta}\quad . \tag{A.15}$$

The result of the contractions of the different tensors obtained from the integrations with the tensors (made from products of gamma matrices) $T^{(M)}$ are given in tables A.1–A.4. For contractions with $T^{(1)}$, $T^{(3)}$, and $T^{(5)}$, $\hat{p} = p'$, while for contractions with $T^{(7)}$, $\hat{p} = p$. The reduction of the gamma matrix algebra has been carried out in $n = 4 - \epsilon$ dimensions and terms of order ϵ^2 were neglected. Only the terms relevant to the computation of X_2 are included. The column header labels the particular tensor $T^{(M)}$, and in parenthesis the Lorentz structure extracted. For example, the top left entry of table A.1 gives -4ϵ for the coefficient of $\not{\epsilon}\not{p}'\not{k}$ in the contraction $k_\alpha \, p'_\beta \, \eta_{\gamma\delta}$ with $T^{(1)\alpha\beta\gamma\delta}$. Blank entries are irrelevant for the computation of X_2. Also $\eta_{\alpha\beta}T^{(11b)\alpha\beta} = (8 - 8\epsilon)\not{\epsilon}\not{k} + \ldots$.

Table A1

	$T^{(1)}(\not{\epsilon}\hat{\not{p}}\not{k})$	$T^{(3)}\ (\not{\epsilon}\hat{\not{p}}\not{k})$	$T^{(5)}(\not{\epsilon}\hat{\not{p}}\not{k})$	$T^{(7)}(\not{\epsilon}\hat{p}\cdot k)$
$k_\alpha\ \hat{p}_\beta\ \eta_{\gamma\delta}$	-4ϵ	$-8+12\epsilon$	$8-4\epsilon$	-2ϵ
$k_\alpha\ \hat{p}_\gamma\ \eta_{\beta\delta}$	$8-12\epsilon$	$8-4\epsilon$	12ϵ	0
$k_\alpha\ \hat{p}_\delta\ \eta_{\beta\gamma}$	$-8+4\epsilon$	4ϵ	$-8+4\epsilon$	2ϵ
$k_\beta\ \hat{p}_\alpha\ \eta_{\gamma\delta}$	4ϵ	$8\ -12\epsilon$	$-8+4\epsilon$	4
$k_\beta\ \hat{p}_\gamma\ \eta_{\alpha\delta}$	-4ϵ	$32\ -4\epsilon$	-4ϵ	0
$k_\beta\ \hat{p}_\delta\ \eta_{\alpha\gamma}$	12ϵ	$8\ -4\epsilon$	$8-12\epsilon$	$8-2\epsilon$
$k_\gamma\ \hat{p}_\alpha\ \eta_{\beta\delta}$	$-8+12\epsilon$	$-8+4\epsilon$	-12ϵ	$8-2\epsilon$
$k_\gamma\ \hat{p}_\beta\ \eta_{\alpha\delta}$	4ϵ	$-32\ +4\epsilon$	4ϵ	2ϵ
$k_\gamma\ \hat{p}_\delta\ \eta_{\alpha\beta}$	$8-4\epsilon$	$-8\ +12\epsilon$	-4ϵ	$4-2\epsilon$
$k_\delta\ \hat{p}_\alpha\ \eta_{\beta\gamma}$	$8-4\epsilon$	-4ϵ	$8-4\epsilon$	0
$k_\delta\ \hat{p}_\beta\ \eta_{\alpha\gamma}$	-12ϵ	$-8\ +4\epsilon$	$-8+12\epsilon$	0
$k_\delta\ \hat{p}_\gamma\ \eta_{\alpha\beta}$	$-8+4\epsilon$	$8\ -12\epsilon$	4ϵ	0
$k_\alpha\ \hat{p}_\beta\ \hat{p}_\gamma\ \hat{p}_\delta/\hat{p}^2$	–	–	2ϵ	0
$k_\beta\ \hat{p}_\alpha\ \hat{p}_\gamma\ \hat{p}_\delta/\hat{p}^2$	–	–	-2ϵ	2
$k_\gamma\ \hat{p}_\alpha\ \hat{p}_\beta\ \hat{p}_\delta/\hat{p}^2$	–	–	-2ϵ	2
$k_\delta\ \hat{p}_\alpha\ \hat{p}_\beta\ \hat{p}_\gamma/\hat{p}^2$	–	–	2ϵ	0

Table A2

	$T^{(1)}(\not\epsilon)$	$T^{(3)}(\not\epsilon)$	$T^{(5)}(\not\epsilon)$	$T^{(7)}(\not\epsilon)$
$\hat{p}_\alpha\ \hat{p}_\beta\ \eta_{\gamma\delta}/\hat{p}^2$	-4ϵ	$8-4\epsilon$	$8-12\epsilon$	$2-\epsilon$
$\hat{p}_\alpha\ \hat{p}_\gamma\ \eta_{\beta\delta}/\hat{p}^2$	$-8-4\epsilon$	$8+4\epsilon$	-4ϵ	$4-\epsilon$
$\hat{p}_\alpha\ \hat{p}_\delta\ \eta_{\beta\gamma}/\hat{p}^2$	$-8+4\epsilon$	$16-12\epsilon$	$-8+4\epsilon$	ϵ
$\hat{p}_\gamma\ \hat{p}_\delta\ \eta_{\alpha\beta}/\hat{p}^2$	$8-12\epsilon$	$8-4\epsilon$	-4ϵ	$2-\epsilon$
$\hat{p}_\beta\ \hat{p}_\delta\ \eta_{\alpha\gamma}/\hat{p}^2$	-4ϵ	$8+4\epsilon$	$-8-4\epsilon$	$4-\epsilon$
$\hat{p}_\beta\ \hat{p}_\gamma\ \eta_{\alpha\delta}/\hat{p}^2$	4ϵ	$32-20\epsilon$	4ϵ	ϵ
$\eta_{\alpha\beta}\ \eta_{\gamma\delta}$	$16-32\epsilon$	$16\ -8\epsilon$	$16-32\epsilon$	$4-4\epsilon$
$\eta_{\alpha\gamma}\ \eta_{\beta\delta}$	$-32+8\epsilon$	$16\ +16\epsilon$	$-32+8\epsilon$	$16-8\epsilon$
$\eta_{\alpha\delta}\ \eta_{\gamma\beta}$	$-32+32\epsilon$	$64\ -72\epsilon$	$-32+32\epsilon$	$4+2\epsilon$
$\hat{p}_\alpha\ \hat{p}_\beta\ \hat{p}_\gamma\ \hat{p}_\delta/(\hat{p}^2)^2$	–	–	-2ϵ	1

Table A3

	$T^{(9)}(\not\epsilon\not k)$	$T^{(10)}(\not\epsilon\not k)$
$k_\alpha\ \eta_{\beta\gamma}$	$8-8\epsilon$	$-8+8\epsilon$
$k_\beta\ \eta_{\alpha\gamma}$	$16-12\epsilon$	$8-16\epsilon$
$k_\gamma\ \eta_{\alpha\beta}$	4ϵ	-4ϵ

Table A4

	$T^{(11a)}(\not\epsilon\not k)$
$\eta_{\alpha\beta}\ k\cdot\epsilon$	$8-10\epsilon$
$k_\alpha\ \epsilon_\beta$	$4-2\epsilon$
$k_\beta\epsilon_\alpha$	-2ϵ

Appendix B. An Integral in Dimensional Regularization

In calculating the anomalous dimension matrix, it is necessary to isolate the infinite piece of Feynman diagrams and extract the coefficient of this infinite piece. Since infinity times a constant is still infinity, this coefficient would be difficult to extract without some way of *regularizing* the infinite integrals encountered. We want to isolate the coefficient of $\frac{1}{\epsilon}$ as $\epsilon \to 0$. So we will do the integrals in $d = 4 - \epsilon$ dimensions and find an expansion in powers of ϵ. In dimensional regularization, both loop momenta and the Dirac matrices are continued to $d = 4 - \epsilon$ dimensions.

A one-loop diagram will give rise to integrals that can be expressed as

$$I(m,n) = \int \frac{d^d k'}{(2\pi)^d} \frac{(k'^2)^r}{[k'^2 - R^2]^m}. \tag{B.1}$$

Rotating to Euclidean space yields

$$I(m,n) = (-1)^{r-m}\ i \int \frac{d^d k}{(2\pi)^d} \frac{(k^2)^r}{[k^2 + R^2]^m}. \tag{B.2}$$

For a spherically symmetric integrand

$$\int d^d k = \Omega_{d-1} \int_0^\infty dk k^{d-1}, \tag{B.3}$$

where Ω_{d-1} is the volume of a $d-1$ dimensional sphere. Noting that

$$\int d^d k e^{-k^2} = \pi^{d/2} = \Omega_{d-1} \int_0^\infty (2kdk)\frac{1}{2}(k^2)^{d/2-1} e^{-k^2}$$

$$= \Omega_{d-1} \frac{1}{2} \Gamma(\frac{d}{2}), \tag{B.4}$$

then,

$$\Omega_{d-1} = \frac{2\pi^{d/2}}{\Gamma(d/2)}. \tag{B.5}$$

Changing the integration from dk to $d(k^2)$ gives

$$I(m,n) = (-1)^{r-m}\, i\frac{\pi^{d/2}}{\Gamma(d/2)} \int_0^\infty \frac{d(k^2)}{(2\pi)^d} \frac{(k^2)^{d/2-1+r}}{[k^2+R^2]^m}. \tag{B.6}$$

Using Schwinger's trick to evaluate

$$\int_0^\infty d(k^2)(k^2)^p(k^2+R^2)^{-q} \tag{B.7}$$

gives

$$\frac{1}{\Gamma(q)}\int_0^\infty ds \int_0^\infty d(k^2)(k^2)^p s^{q-1} e^{-s(k^2+R^2)}$$

$$= \frac{1}{\Gamma(q)}\int_0^\infty ds s^{q-1} e^{-sR^2} s^{-(p+1)}\Gamma(p+1)$$

$$= (R^2)^{p-q+1}\frac{\Gamma(p+1)}{\Gamma(q)}\Gamma(q-p-1). \tag{B.8}$$

So that finally we arrive at

$$I(m,n) = \frac{i}{(16\pi^2)^{d/4}}(-1)^{r-m}(R^2)^{r-m+d/2}\frac{\Gamma(r+d/2)\Gamma(m-r-d/2)}{\Gamma(d/2)\Gamma(m)}. \tag{B.9}$$

Our two-loop integrals can be put into the form where the above result, used twice, will complete the loop-momenta integration.

Some gamma matrix identities needed to reduce the gamma matrix structure of our Feynman diagrams are (in d dimensions):

$$\gamma_\mu \gamma^\mu = d\mathbf{1}, \qquad (B.10a)$$

$$\gamma_\mu \gamma^\alpha \gamma^\mu = (2-d)\gamma^\alpha, \qquad (B.10b)$$

$$\gamma_\mu \gamma^\alpha \gamma^\beta \gamma^\mu = 4g^{\alpha\beta}\mathbf{1} + (d-4)\gamma^\alpha \gamma^\beta, \qquad (B.10c)$$

$$\gamma_\mu \gamma^\alpha \gamma^\beta \gamma^\gamma \gamma^\mu = -2\gamma^\gamma \gamma^\beta \gamma^\alpha - (d-4)\gamma^\alpha \gamma^\beta \gamma^\gamma. \qquad (B.10d)$$

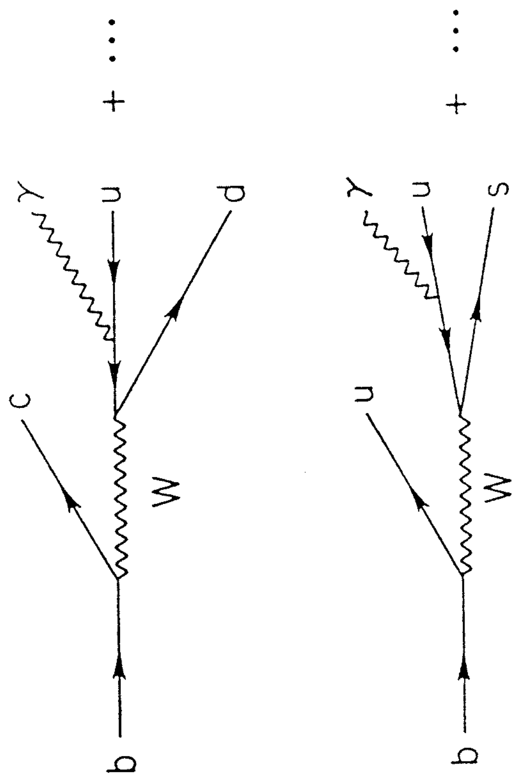

FIGURE 1

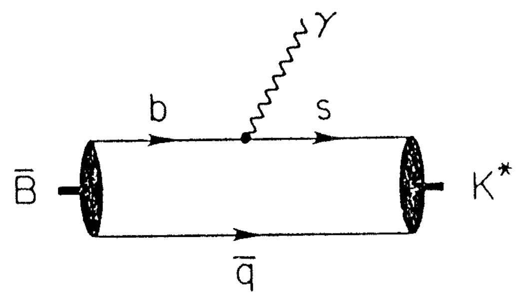

FIGURE 2

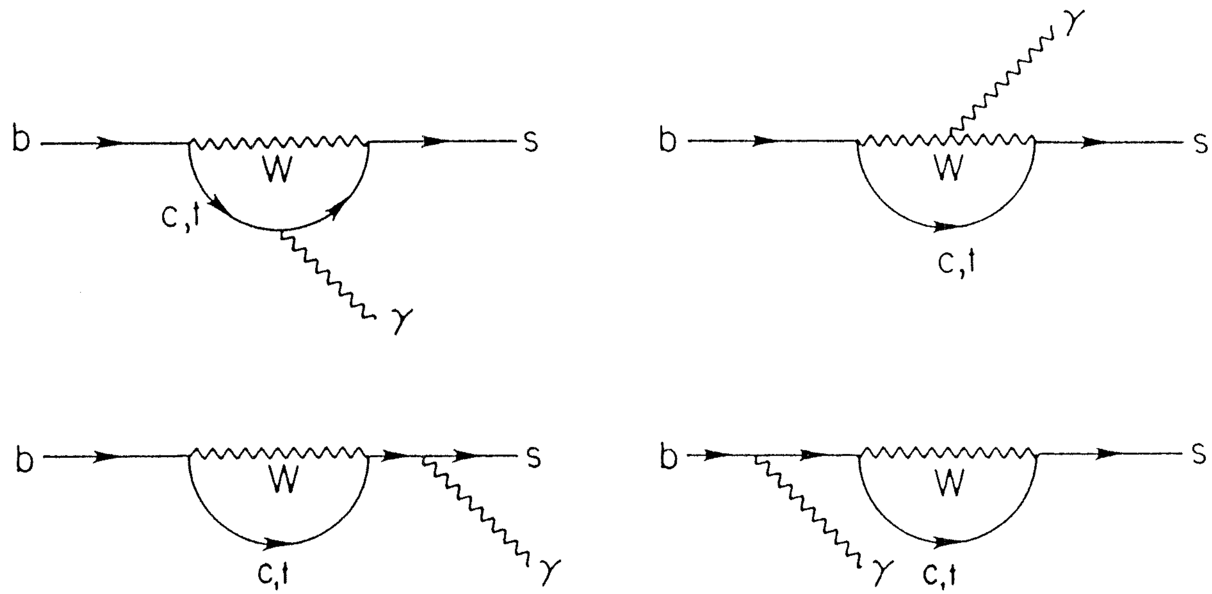

FIGURE 3

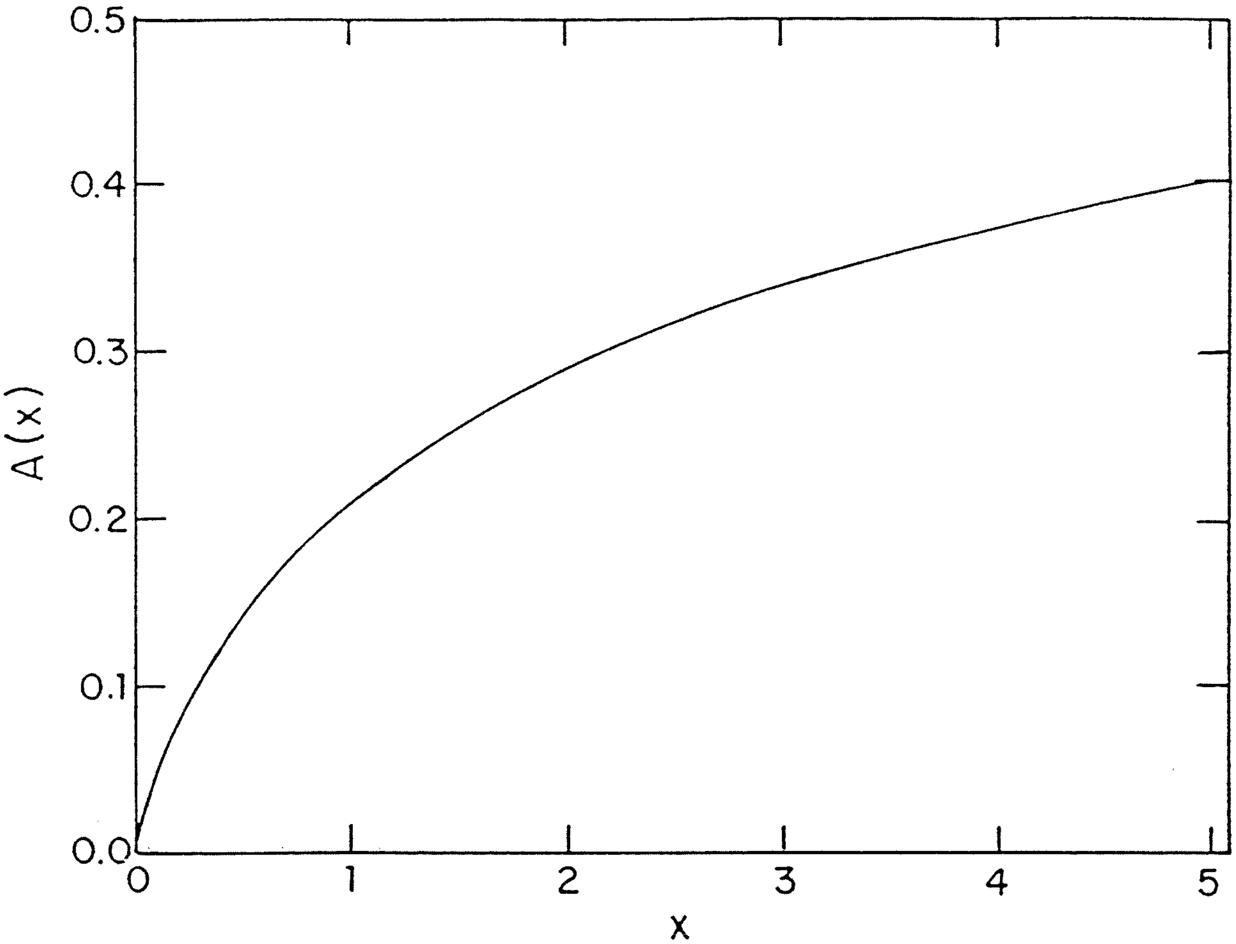

FIGURE 4

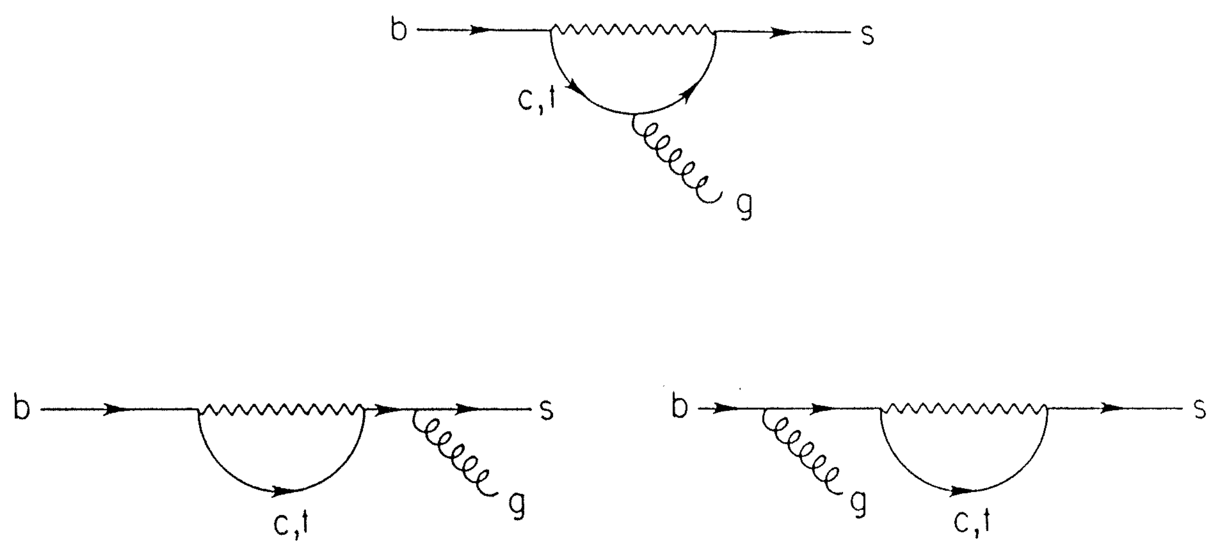

FIGURE 5

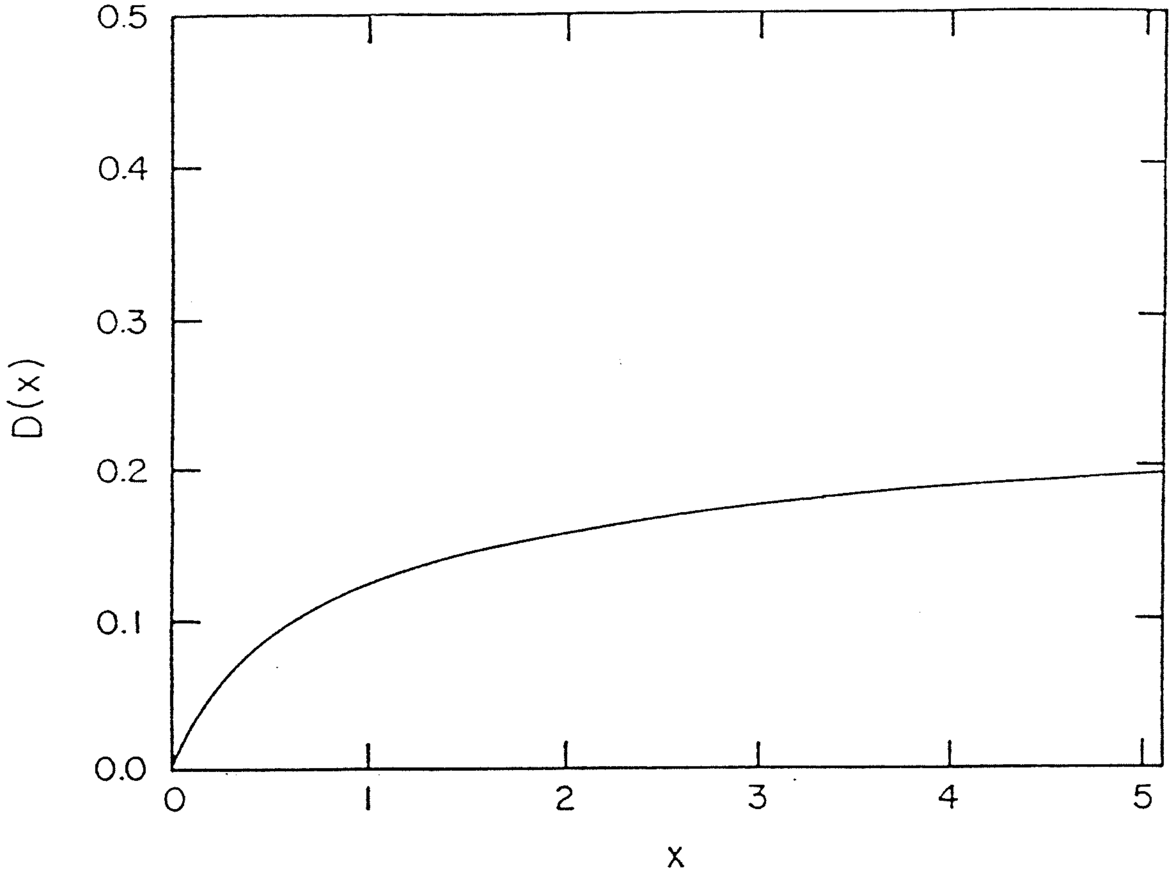

FIGURE 6

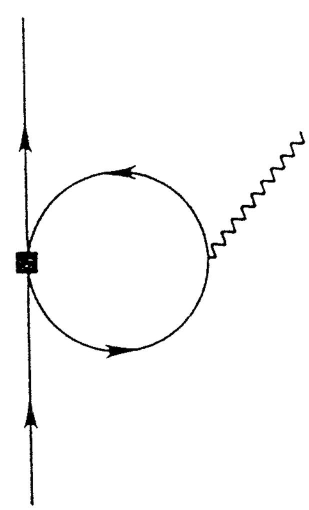

FIGURE 7

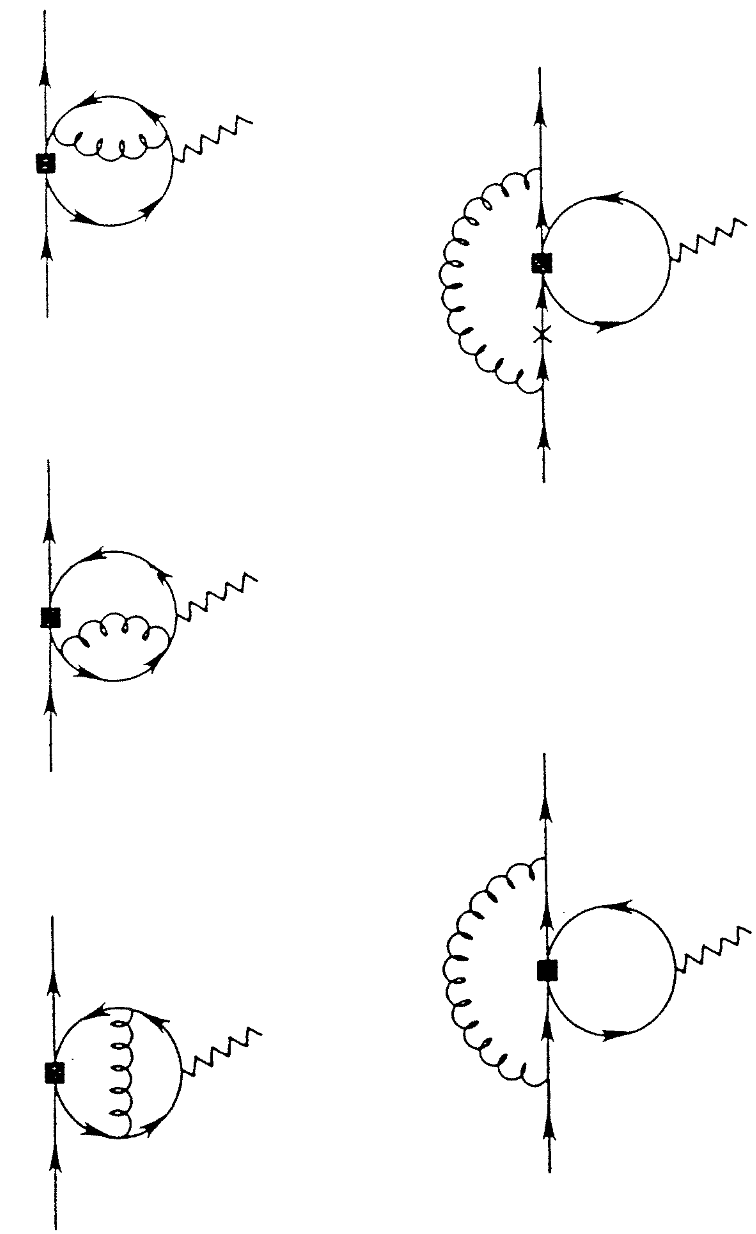

FIGURE 8

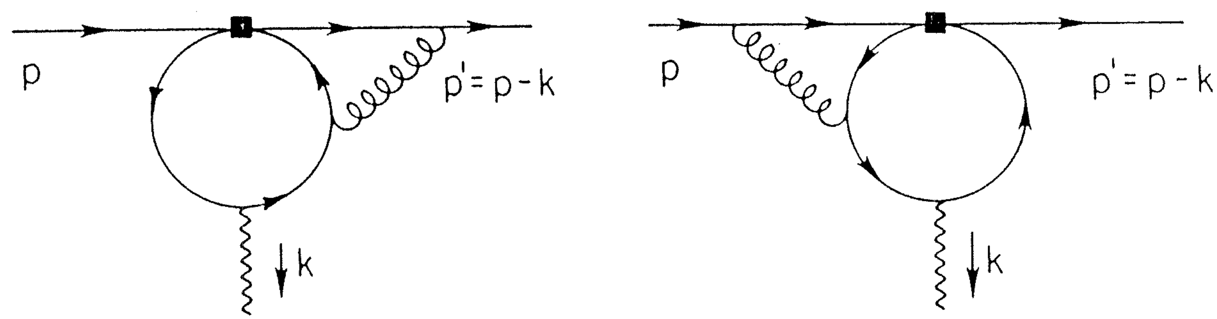

FIGURE 9

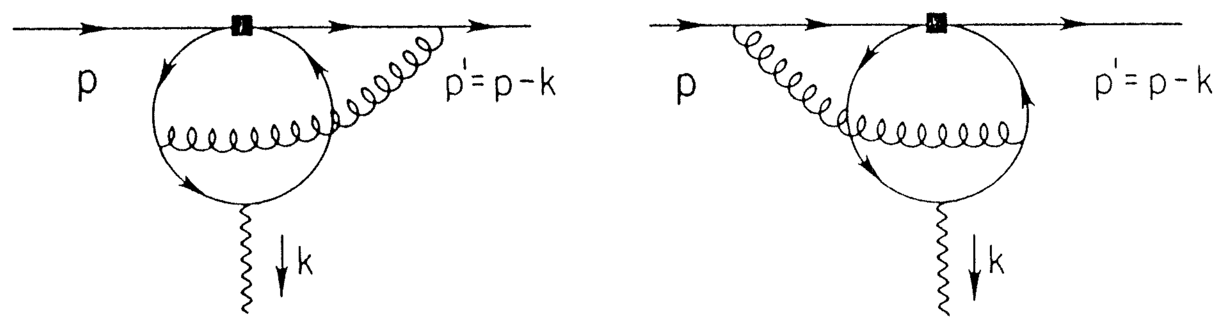

FIGURE 10

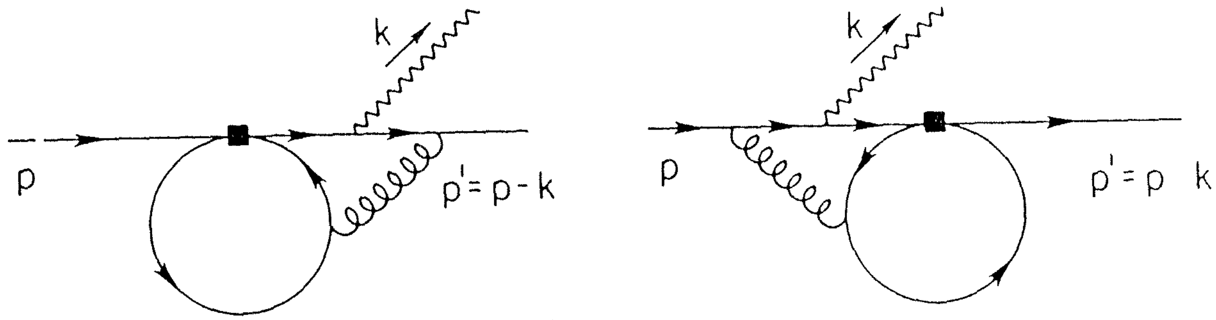

FIGURE 11

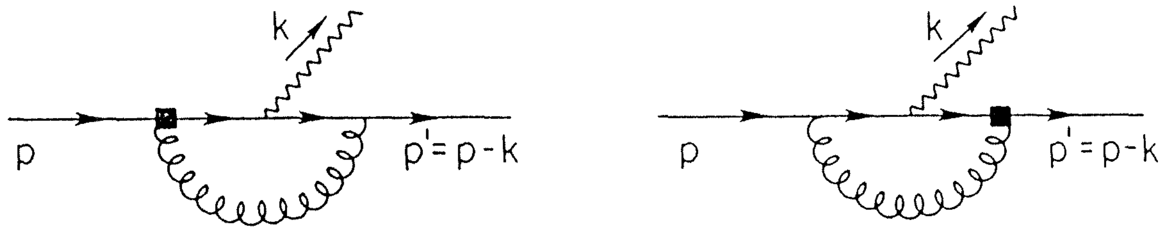

FIGURE 12

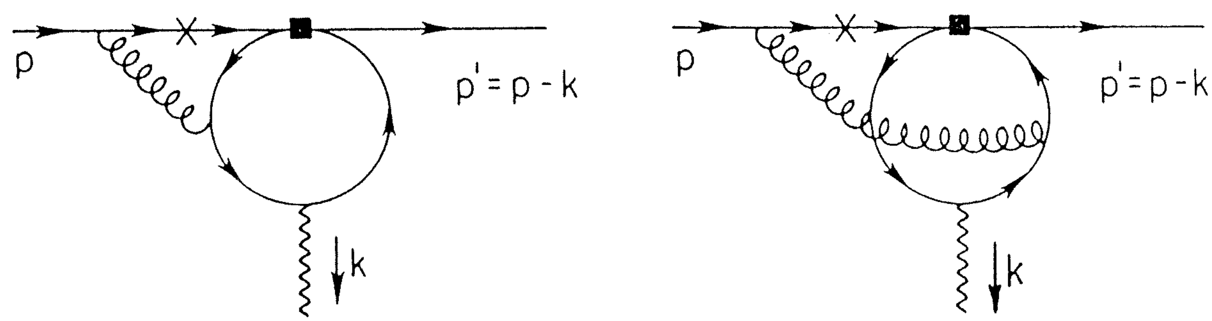

FIGURE 13

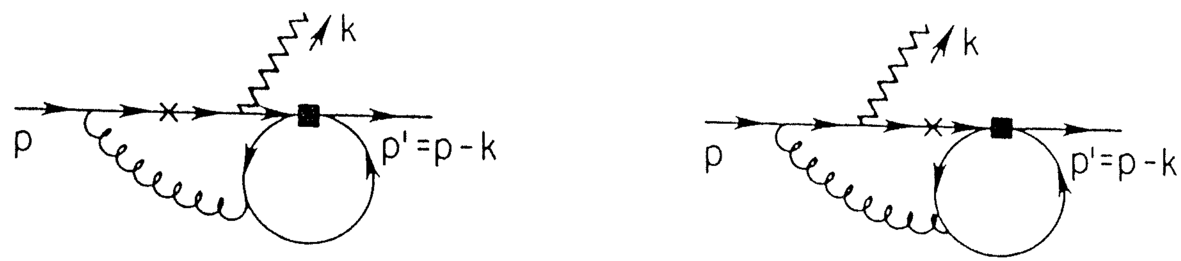

FIGURE 14

FIGURE 15

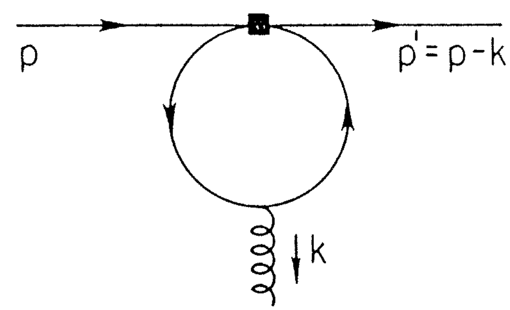

FIGURE 16

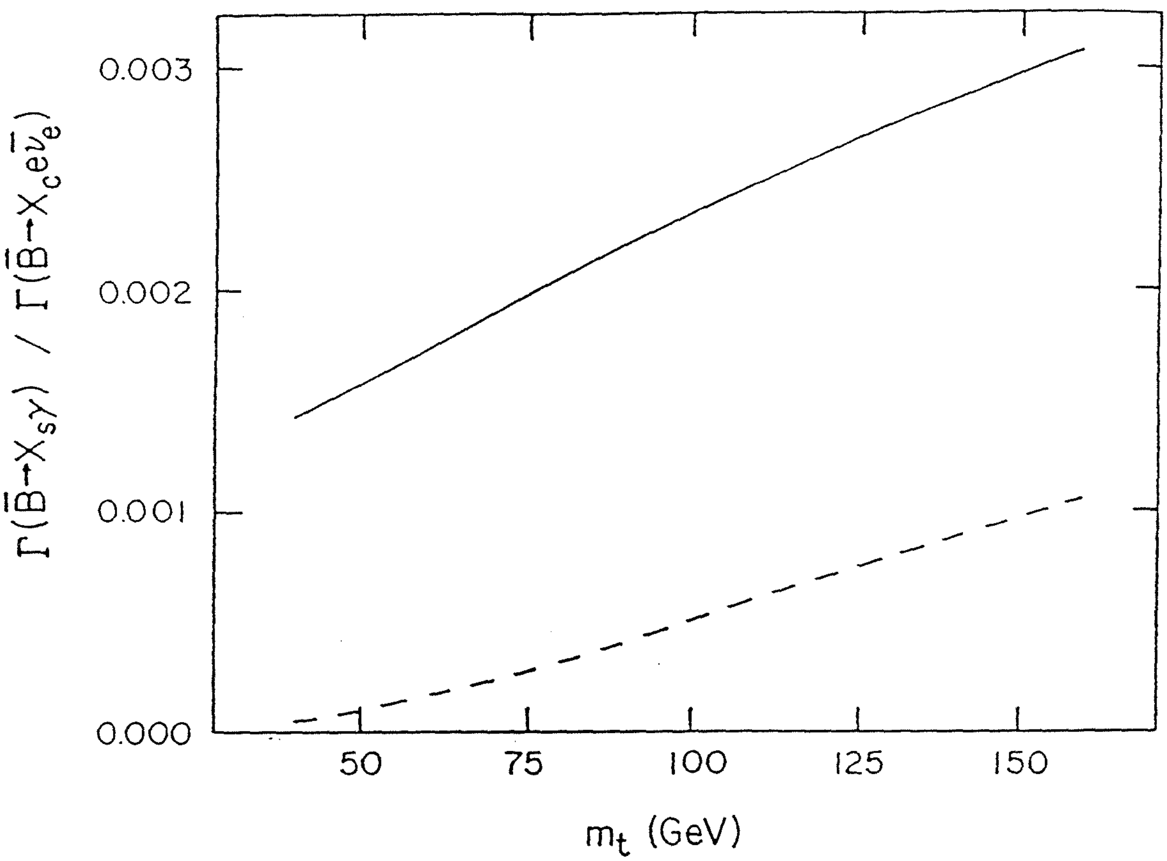
0.003
0.002
0.001
0.000
50
75
100
125
150
m_t (GeV)
$\Gamma(\bar{B}\to X_s\gamma)$ / $\Gamma(\bar{B}\to X_c e\bar{\nu}_e)$

FIGURE 17